IN-SILICO, SYNTHESIS AND CHARACTERIZATION SCREENING OF SOME IMIDAZOLE DERIVATIVES FOR POTENTIAL ANTIHYPERTENSIVE ACTIVITY

BY

NWONU EBERE GIFT

PHA1908548

SUPERVISED BY:

DR. ISONAH UNUIGBE

A PROJECT SUBMITTED TO THE DEPARTMENT OF PHARMACEUTICAL CHEMISTRY IN PARTIAL FULFILMENT OF THE REQUIREMENT FOR THE AWARD OF DOCTOR OF PHARMACY (PHARM.D) DEGREE OF THE UNIVERSITY OF BENIN, BENIN CITY, EDO STATE.

NOVEMBER, 2025

CERTIFICATION

This is to certify that this project work was carried out by **NWONU EBERE GIFT** in the Department of Pharmaceutical Chemistry, Faculty of Pharmacy, University of Benin, Benin City, Edo State.

NWONU EBERE GIFT	**DATE**
STUDENT	
DR. ISONAH UNUIGBE	**DATE**
PROJECT SUPERVISOR	
DR. VINCENT IMIEJE	**DATE**
HEAD OF DEPARTMENT	

DEDICATION

This project work is dedicated to the Almighty God for His grace and faithfulness in my life.

ACKNOWLEDGEMENT

To God Almighty, from whom all blessings flow, I am grateful for the strength He has provided throughout this academic journey.

I would like to express my deepest gratitude to my project supervisor, Dr. Isonah Inuigbe for his unwavering guidance and invaluable advice throughout this work. His expertise and insights have been fundamental to the success of this work.

I extend my heartfelt gratitude to my family, with special thanks to my mother, **Mrs. Ebere Nwonu** whose support and encouragement have been my pillars of strength. I am also deeply grateful to my siblings for their constant care and the various forms of support they have provided, which have been instrumental to my success.

My heartfelt appreciation goes to my friends Mercy, Divine, Ayomide, Elizabeth, and Aniebet, to my colleagues, and to everyone who supported me during the course of this project.

Finally, I am also grateful to my project partners for his collaboration and the countless hours dedicated to this work.

TABLE OF CONTENTS

LIST OF FIGURES

LIST OF TABLES

ABSTRACT

Cardiovascular disorders, particularly hypertension, continue to pose major health challenges worldwide, necessitating the search for new therapeutic agents with improved efficacy and safety. Imidazole-based compounds have gained attention due to their diverse pharmacological profiles, including notable antibacterial, antifungal and antihypertensive properties.

This study employed a computational screening approach to evaluate selected imidazole derivatives for potential antihypertensive activity, followed by the synthesis of a lead derivative (2,4,5-triphenyl-1H-imidazole). Molecular docking was conducted using PyRx (AutoDock Vina) to predict binding affinities and interaction profiles with key hypertension-related protein targets1O86, 4ZUD, 5XPR and 6L88).

Several screened derivatives demonstrated strong binding affinities comparable to or higher than the reference drug, suggesting potential inhibitory activity through similar interaction mechanisms at the active site residues. In particular, 2,4,5-triphenyl-1H-imidazole, 1-benzoyl-4,5-diphenyl-1H-imidazole, and 2-(2-methoxyphenyl)-4,5-diphenyl-1H-imidazole showed the most favorable binding energies and stable protein–ligand interactions across all target proteins. ADMET profiling further indicated acceptable pharmacokinetic behavior for these candidates.

The synthesized 2,4,5-triphenyl-1H-imidazole was obtained in a yield of 81.28% and was subjected to preliminary characterization, exhibiting a melting point of 269–272 °C.. The findings highlight promising imidazole structural features with potential antihypertensive relevance and support further synthesis, and biological evaluation of these compounds to advance drug development in hypertension management.

CHAPTER ONE

INTRODUCTION AND LITERATURE REVIEW

1.1 Introduction

Hypertension remains one of the foremost global public-health challenges of the 21st century. Despite advances in cardiovascular pharmacotherapy, hypertension continues to contribute significantly to morbidity and mortality via its role in cardiovascular disease, stroke, renal failure and other end-organ damage. Conventional antihypertensive agents have undoubtedly improved outcomes; however, limitations persist. These include variable patient responses, adverse-effect profiles, drug-resistance mechanisms, and in many under-resourced settings, issues of cost, compliance and access. Hence, there remains a compelling need for novel chemical entities with improved efficacy, safety, affordability and mechanistic diversity.

In medicinal-chemistry efforts to address such unmet needs, heterocyclic compounds have emerged as privileged motifs in drug design for cardiovascular, metabolic and inflammatory disorders. Among these, the imidazole ring stands out for its versatility: it confers favourable physicochemical characteristics and is present in biologically important molecules and numerous drug. Indeed, recent reviews have emphasized that imidazole-derived compounds are increasingly explored across disease areas including antimicrobial, anticancer, anti-inflammatory and even antihypertensive applications. For example, a mini-review states that “derivatives of imidazole have occupied a critical place in the field of medicinal chemistry” and extend to antihypertensive properties. (Ibrahim et al. 2024). Moreover, imidazole-based heterocycles have been specifically identified as “heterocyclic moieties for the antihypertensive activity” in several heterocycle-focused surveys. (Singh 2017). Several clinically used drugs, such as losartan and

eprosartan, contain the imidazole ring as an active pharmacophore responsible for their antihypertensive effects. With advances in computational chemistry, in silico methods now provide valuable tools for predicting molecular interactions, pharmacokinetic properties, and toxicity of new compounds prior to synthesis, thereby reducing time and cost in drug discovery.

This study therefore integrates in silico molecular screening with laboratory synthesis and characterization of an imidazole derivative, with the aim of identifying potential candidates for antihypertensive drug development.

1. 2 Computer-Aided Drug Design

Computer-Aided Drug Design (CADD) is a modern approach that uses computational tools to identify and optimize potential drug candidates before laboratory synthesis and testing. It supports the discovery and optimization of small-molecule therapeutics by modelling the interactions between drug candidates and biological targets (Agarwal et al. 2025). By simulating molecular interactions, CADD allows scientists to screen thousands of compounds virtually and select the most promising candidates for synthesis and testing, CADD enables researchers to predict binding affinities, assess drug-likeness (including ADMET: absorption, distribution, metabolism, excretion and toxicity), and optimize lead compounds prior to synthesis. In doing so, CADD can significantly reduce the time, cost and experimental burden traditionally associated with drug development (Lakshmi et al 2025).

1.2.1 Types of Computer-Aided Drug Design

Computer-Aided Drug Design (CADD) broadly encompasses two principal approaches. Both methods employ computational tools to identify, optimize, and predict potential therapeutic compounds but differ in the type of information they rely upon.

1. Structure-Based Drug Design (SBDD)

SBDD uses the three-dimensional (3D) structure of a biological target typically an enzyme or receptor to guide drug design. When the target's crystal structure or homology model is known, molecular docking, molecular dynamics simulations, and pharmacophore modelling can be applied to predict how ligands interact within the active site (Lionta *et al.,* 2014). These three-dimensional (3D) structures of biological macromolecules are usually determined by X-ray crystallography, NMR spectroscopy, or cryo-electron microscopy. This method helps identify binding conformations, key intermolecular interactions, and estimate binding affinities, thus reducing experimental trial-and-error.

2. Ligand-Based Drug Design (LBDD)

LBDD is applied when the 3D structure of the biological target is unknown. It relies on information derived from known active ligands to predict new molecules with similar pharmacophoric or physicochemical properties. Techniques used include quantitative structure–activity relationship (QSAR) modelling, pharmacophore mapping, and similarity searching (Leelananda & Lindert, 2016). LBDD is particularly useful in hit-to-lead optimization when structural data are limited but biological assay results for analogues are available.

3. Hybrid and De Novo Design Approaches

Modern drug discovery often combines both approaches, termed integrative or hybrid CADD, which leverages structural data and ligand information simultaneously. De novo design, a subset of SBDD, involves constructing new molecules directly within the active site of the

target protein, guided by binding-energy calculations and synthetic feasibility predictions. (Schneider & Fechner, 2005).

1.3 Molecular docking

Molecular docking, one of the most widely used computational techniques in Computer-Aided Drug Design (CADD) for predicting the preferred orientation of a small molecule (ligand) when bound to a biological macromolecule (receptor or enzyme). The goal of docking is to estimate both the binding mode and the binding affinity of potential drug candidates, thereby facilitating the identification of molecules with favorable interactions before synthesis and experimental validation (Meng *et al.,* 2011; Lionta *et al.,* 2014).

The fundamental principle of molecular docking is based on the "lock-and-key" or "induced-fit" models of enzyme–substrate interaction, where the ligand fits into the active site of the receptor to form a stable complex. The docking process involves two major components: a search algorithm, which explores the possible binding conformations of the ligand within the active site, and a scoring function, which evaluates the binding affinity and stability of each predicted pose (Trott & Olson, 2010). A good docking model aims to identify the binding mode that corresponds to the lowest free energy of binding, reflecting the most favorable ligand–receptor interaction (Forli *et al.,* 2016).

Two major docking paradigms exist: rigid docking, where both receptor and ligand are treated as rigid bodies, and flexible docking, which allows torsional or side-chain adjustments to better simulate biological conditions. Flexible docking is computationally intensive but yields more realistic predictions of binding conformations and energetics. In recent years, induced-fit docking (IFD) and ensemble docking have gained prominence for

addressing receptor flexibility by using multiple protein conformations (Moitessier *et al.,* 2008).

Over the past decades, docking has become an indispensable tool in structure-based drug design, particularly for understanding the interactions of potential inhibitors with therapeutic targets. Software packages such as AutoDock, AutoDock Vina, GOLD, and Glide are widely used for virtual screening and lead optimization (Pagadala et al., 2017). These tools integrate sophisticated scoring algorithms that account for electrostatic forces, hydrogen bonding, hydrophobic contacts, and van der Waals interactions to predict the strength and stability of ligand binding.

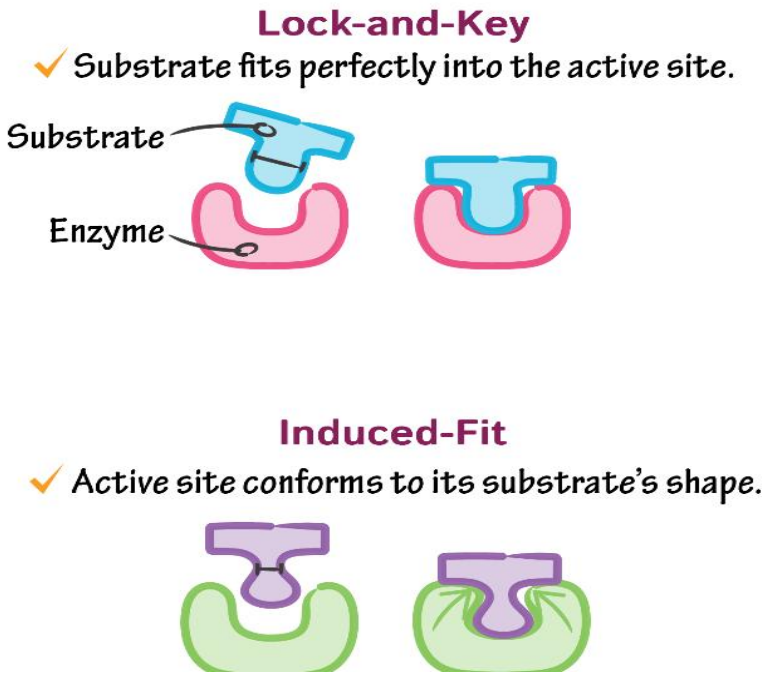

Figure 1.1 Showing the fundamental principles of molecular docking

1.3.1 Application of Molecular Docking in Drug Discovery

Molecular docking has become a central tool in rational drug discovery due to its ability to model and predict molecular interactions at atomic resolution. It facilitates understanding of

how small molecules interact with biological targets, guiding the design and optimization of novel therapeutics. Below are the major applications of molecular docking in modern drug discovery and development.

1. Virtual Screening of Drug Candidates

Molecular docking enables virtual screening (VS) of large chemical libraries to identify compounds with high binding affinity to specific biological targets. It drastically reduces the time and cost associated with experimental screening by narrowing down thousands of compounds to a few promising hits. This approach has been widely used in identifying inhibitors for enzymes, receptors, and viral proteins (Meng *et al.,* 2011; Pagadala *et al.,* 2017).

2. Lead Optimization

Once potential hits are identified, docking assists in lead optimization by evaluating structural modifications that improve binding affinity, selectivity, or pharmacokinetic properties. By simulating how structural changes affect ligand–receptor interactions, researchers can design analogs with enhanced potency and minimized off-target effects (Trott & Olson, 2010).

3. Elucidation of Structure–Activity Relationship (SAR)

Docking provides insights into the structure–activity relationship (SAR) of compounds by correlating molecular structures with their biological activities. Through visualizing

interactions such as hydrogen bonding, hydrophobic effects, and metal coordination, scientists can identify critical functional groups responsible for bioactivity (Forli *et al.,* 2016).

4. Repurposing of Existing Drugs

   Molecular docking is increasingly used for drug repurposing, the identification of new therapeutic targets for approved or investigational drugs. By screening existing drug libraries against novel targets, docking can uncover unanticipated activities, thus accelerating clinical translation and reducing development risks (Santos *et al.,* 2019).

1.4 Hypertension

Hypertension, commonly referred to as high blood pressure, is a chronic medical condition characterized by a persistent elevation of systolic and/or diastolic blood pressure above the normal physiological range. According to the World Health Organization (WHO), hypertension is diagnosed when systolic blood pressure (SBP) is ≥140 mmHg or diastolic blood pressure (DBP) is ≥90 mmHg, based on repeated measurements (WHO, 2023). It remains one of the most prevalent non-communicable diseases globally and a leading modifiable risk factor for cardiovascular morbidity and mortality (Singh et al. 2000; Kearney et al. 2005).

Hypertension is often termed the “silent killer” because it typically remains asymptomatic until significant organ damage occurs. Prolonged uncontrolled blood pressure leads to serious complications, including stroke, coronary artery disease, heart failure, chronic kidney disease, and peripheral vascular disease (Mills *et al.,* 2020).

1.4.1 Epidemiology of Hypertension

Globally, hypertension affects approximately 1.28 billion adults aged 30–79 years, with nearly 46% unaware of their condition (WHO, 2023). The burden is disproportionately higher in low-

and middle-income countries, including many regions of sub-Saharan Africa, due to limited awareness, diagnostic infrastructure, and access to quality care (Mills *et al.,* 2020). According to the Global Burden of Disease Study, hypertension accounts for over 10 million deaths annually, making it the most significant preventable cause of cardiovascular mortality worldwide (GBD, 2020).

In Nigeria, the burden of hypertension has risen sharply over the past four decades. The pooled prevalence increased from 8.9% in the 1990s to approximately 28.9% in recent years, reflecting a significant epidemiological transition toward non-communicable diseases (Adeloye et al. 2015). Hypertension-related conditions now represent a major cause of hospital admissions in the country, accounting for 20.5% to 69.6% of total medical admissions in various regional studies, with case fatality rates reported as high as 42.9% (Ogah et al. 2012).

1.4.2 Etiology and Risk Factors

An interplay of genetic, environmental, physiological, and behavioral factors that disturb the normal mechanisms regulating vascular tone, cardiac output, and renal function are often responsible for high blood pressure. The etiology of hypertension can be broadly categorized into primary (essential) hypertension, which accounts for about 90–95% of cases, and secondary hypertension, which arises from identifiable underlying pathologies.

1. Primary (Essential) Hypertension

Primary hypertension develops gradually without a single identifiable cause but results from the cumulative influence of hereditary predisposition and environmental exposures that alter vascular homeostasis. It is largely age-related and multifactorial, reflecting dysfunction in

several interdependent systems including the renin–angiotensin–aldosterone system (RAAS), sympathetic nervous system (SNS), and endothelial regulation.

Genetic factors play a fundamental role in blood pressure variability. Twin and family studies demonstrate heritability estimates between 30–50%, implicating multiple gene variants that modulate sodium handling, vascular tone, and hormonal regulation (Ehret & Caulfield, 2013). Polymorphisms in genes encoding components of the RAAS such as angiotensinogen (AGT), angiotensin-converting enzyme (ACE), and angiotensin II receptor type 1 (AGTR1) have been associated with elevated blood pressure and increased cardiovascular risk (Fajar *et al.,* 2019). In addition, genetic variations influencing renal sodium reabsorption and sympathetic activity contribute to interindividual susceptibility.

Renin–angiotensin–aldosterone system dysregulation represents a key pathogenic pathway. Overactivation of RAAS leads to excessive production of angiotensin II, a potent vasoconstrictor that promotes sodium retention, vascular hypertrophy, and increased systemic resistance (Carretero & Oparil, 2000). Aldosterone further amplifies the effect by enhancing sodium reabsorption in renal tubules, thereby increasing intravascular volume. Chronic RAAS stimulation contributes to endothelial dysfunction and vascular remodeling.

Sympathetic nervous system (SNS) hyperactivity is another crucial contributor. Heightened sympathetic outflow elevates heart rate, myocardial contractility, and peripheral vascular resistance. Persistent SNS activation may result from psychosocial stress, obesity, or insulin resistance, and it promotes the release of catecholamines such as norepinephrine, which constrict arterioles and stimulate renin secretion (Grassi *et al.,* 2009). These effects create a self-reinforcing loop between the SNS and RAAS, maintaining elevated arterial pressure.

Endothelial dysfunction further accentuates hypertension by impairing vasodilator mechanisms. Normally, endothelial cells regulate vascular tone through the balanced release of vasodilators (nitric oxide and prostacyclin) and vasoconstrictors (endothelin-1 and thromboxane). In hypertensive individuals, oxidative stress, inflammation, and reduced nitric oxide bioavailability disrupt this equilibrium, resulting in increased vascular resistance and stiffness (Taddei *et al.,* 2000). Moreover, low-grade inflammation characterized by elevated C-reactive protein and cytokines such as interleukin-6 contributes to endothelial damage and atherogenesis.

Renal mechanisms also play a pivotal role. The kidney maintains long-term blood pressure control through sodium excretion and volume regulation. Impaired renal function—either structural or functional—leads to sodium retention, extracellular fluid expansion, and volume-dependent hypertension. Guyton's pressure-natriuresis theory posits that a rightward shift in the renal function curve due to reduced sodium excretion capacity sustains elevated blood pressure (Guyton, 1991). Even minor defects in nephron number or function can trigger maladaptive neurohormonal activation that perpetuates hypertension.

Metabolic and lifestyle factors significantly modulate the expression of genetic predisposition. High dietary sodium intake, low potassium consumption, excessive alcohol use, obesity, and physical inactivity contribute independently to hypertension risk (Appel *et al.,* 2011). Obesity, in particular, induces insulin resistance, stimulates SNS and RAAS activity, and promotes renal sodium reabsorption. Adipose tissue also acts as an endocrine organ, secreting adipokines such as leptin and resistin that influence vascular tone and inflammation. Insulin resistance further exacerbates hypertension through enhanced sympathetic drive and impaired nitric oxide-mediated vasodilation.

2. Secondary Hypertension

Secondary hypertension results from specific, often treatable, underlying causes. It accounts for approximately 5–10% of all hypertension cases and should be suspected in patients with abrupt onset, resistant hypertension, or onset at a young age.

Renal causes are the most common, encompassing chronic kidney disease (CKD), glomerulonephritis, and renovascular hypertension. In renal parenchymal disease, nephron loss reduces sodium excretion, increasing fluid retention and activating RAAS. **Renovascular** hypertension, caused by renal artery stenosis due to atherosclerosis or fibromuscular dysplasia, leads to ischemia-induced renin release and secondary hyperaldosteronism (Safar *et al.,* 2004).

Endocrine disorders also contribute substantially. Primary hyperaldosteronism (Conn's syndrome) involves excessive aldosterone secretion independent of renin, resulting in sodium retention, hypokalemia, and volume expansion. Cushing's syndrome, characterized by chronic glucocorticoid excess, increases vascular sensitivity to catecholamines and stimulates mineralocorticoid receptors. Pheochromocytoma, a catecholamine-secreting tumor of the adrenal medulla, causes episodic hypertension due to surges in epinephrine and norepinephrine. Hypothyroidism and hyperthyroidism can both affect vascular resistance and cardiac output, altering blood pressure dynamics.

Cardiovascular abnormalities such as coarctation of the aorta produce mechanical obstruction to blood flow, raising proximal arterial pressure. Additionally, sleep apnea and chronic hypoxia induce intermittent sympathetic activation and oxidative stress, contributing to sustained hypertension.

Pharmacological and chemical factors are increasingly recognized in secondary hypertension. Nonsteroidal anti-inflammatory drugs (NSAIDs), oral contraceptives, corticosteroids, cyclosporine, and certain antidepressants can elevate blood pressure through several mechanisms including sodium retention, altered prostaglandin synthesis, or increased vascular reactivity. Excessive intake of caffeine, licorice, or illicit substances such as cocaine and amphetamines has similar effects (Whelton *et al.,* 2018).

1.4.4 Pathophysiology of Hypertension

Blood pressure regulation involves the coordinated actions of the heart, kidneys, blood vessels, and neurohormonal systems to maintain tissue perfusion. Hypertension develops when these regulatory systems become dysregulated, leading to a sustained elevation in arterial pressure. These systems do not act in isolation; rather they form a network of maladaptive responses that sustain hypertensive states and lead to target-organ damage.

The endothelium lining blood vessels plays a pivotal role in maintaining vascular tone, fluidity, and structure. A healthy endothelium releases vasodilators (notably nitric oxide – NO) and vasoconstrictors (such as endothelin - 1) in a tightly controlled balance. In hypertension, endothelial dysfunction emerges early and may both contribute to and result from persistently elevated blood pressure. Evidence indicates that hypertensive individuals exhibit reduced NO bioavailability, often due to oxidative stress, decreased endothelial NO synthase (eNOS) function or co-factor availability, and increased reactive oxygen species (ROS) that scavenge NO (Ambrosino *et al.,* 2022; Taylor 2001). This shift leads to impaired vasodilator responses and unopposed vasoconstrictor influences, contributing to increased peripheral vascular resistance. Moreover, endothelial cells under stress shift toward a pro-inflammatory, pro-thrombotic phenotype, with elevated production of endothelin-1, thromboxane, adhesion molecules and

growth factors, promoting vascular remodelling and stiffening of resistance arteries (Ambrosino *et al.,* 2022).

As the arterial wall stiffens and the vasodilatory capacity diminishes, the vascular system contributes directly to elevated systolic arterial pressure and pulse pressure. The vascular dysfunction is not only a consequence of hypertension: it can precede and contribute to the development of sustained hypertension, thus creating a "vicious cycle" between endothelial pathology and elevated pressure (Higashi & Chayama, 2002; Ambrosino *et al.,* 2022).

The kidney plays a vital role in long-term regulation of arterial pressure through sodium and water balance, maintaining extracellular fluid volume. Normally, increased blood pressure promotes renal sodium excretion (pressure-natriuresis), which restores normal pressure levels. However, in hypertension, this mechanism becomes impaired as the pressure-natriuresis curve shifts rightward, meaning higher pressures are needed to achieve the same sodium output indicating altered renal function or maladaptive neurohormonal regulation (Kim, 2024). Deficient sodium excretion results in fluid retention, expanding blood volume and cardiac output, thereby increasing vascular load and resistance (Taylor, 2001). Structural kidney changes such as nephron loss, glomerular hypertension, and endothelial injury further impair filtration and autoregulation, establishing a feedback loop of renal dysfunction and elevated pressure (Ritz *et al.,* 1993).

Neurohormonal mechanisms, particularly the sympathetic nervous system (SNS) and renin–angiotensin–aldosterone system (RAAS), are central to hypertension development. Enhanced sympathetic activity increases heart rate, vasoconstriction, and sodium retention (Medscape, 2023). Concurrently, RAAS activation produces angiotensin II, which drives vasoconstriction,

aldosterone secretion, vascular remodelling, and inflammation (Raina *et al.,*2020). Both systems reinforce each other—angiotensin II stimulates sympathetic output, while SNS activity promotes renin release—creating persistent hypertension and progressive vascular and renal damage (Saxena *et al.,* 2018).

1.4.6 Signs and Symptoms

Most individuals with elevated blood pressure are unaware of their condition, as the disease progresses insidiously over several years (Whelton *et al.,* 2018). When symptoms do manifest, they are usually nonspecific and may include headache, particularly in the occipital region on awakening, dizziness, palpitations, blurred vision, fatigue, and epistaxis (Carretero & Oparil, 2000). Severe or malignant hypertension, however, can present with blurred vision, chest pain, dyspnea, confusion, or epistaxis, often indicating acute end-organ involvement such as hypertensive encephalopathy, heart failure, or retinal hemorrhage (Carey *et al.,* 2018).

Clinical signs detectable on examination include elevated arterial pressure on repeated measurements, displaced apical impulse, retinal hemorrhages or exudates, and renal impairment indicated by proteinuria or elevated serum creatinine. Hypertension frequently lacks early symptoms, routine blood-pressure screening is essential for timely diagnosis and prevention of complications (WHO, 2023).

1.4.7 Hypertensive Crisis

A severe and acute elevation in blood pressure that poses an imminent threat to organ integrity and life, clinically defined as a systolic blood pressure (SBP) ≥180 mmHg and/or diastolic blood pressure (DBP) ≥120 mmHg (Whelton *et al.,* 2018). Hypertensive crisis is broadly classified into

two categories hypertensive urgency and hypertensive emergency based on the presence or absence of target-organ damage (Peixoto, 2015).

Hypertensive urgency occurs when there is a marked increase in blood pressure without acute or progressive end-organ injury. Patients may present with nonspecific symptoms such as severe headache, dizziness, shortness of breath, palpitations, or epistaxis, but diagnostic investigations reveal no evidence of organ dysfunction. Management typically involves the gradual reduction of blood pressure over 24–48 hours using oral antihypertensive medications and close outpatient follow-up to prevent progression to emergency states (Pinna *et al.,* 2020).

In contrast, hypertensive emergency is characterized by severely elevated blood pressure accompanied by evidence of acute target-organ damage to vital organs such as the brain, heart, kidneys, or retina. Clinical manifestations vary depending on the affected system and may include hypertensive encephalopathy, intracerebral hemorrhage, acute coronary syndrome, acute left ventricular failure with pulmonary edema, aortic dissection, or acute renal failure (Vilela-Martin *et al.,* 2011). Hypertensive emergencies demand immediate hospitalization and parenteral antihypertensive therapy to reduce mean arterial pressure by no more than 25% within the first hour, preventing ischemic complications due to abrupt perfusion decline (Whelton *et al.,* 2018).

1.4.8 Non-Pharmacological Management of Hypertension

Lifestyle and behavioral interventions aimed at reducing blood pressure and improving cardiovascular health with or without the immediate use of medication. These measures form the foundation of hypertension prevention and treatment, particularly in individuals with prehypertension or stage 1 hypertension (Whelton *et al.,* 2018). They not only lower blood

pressure but also enhance the effectiveness of antihypertensive drugs and reduce overall cardiovascular risk (Carey *et al.,* 2022).

1. Dietary Modifications

Diet plays a crucial role in blood pressure regulation. The Dietary Approaches to Stop Hypertension (DASH) diet remains one of the most effective interventions. It emphasizes the consumption of fruits, vegetables, whole grains, lean proteins, and low-fat dairy products while limiting saturated fats, cholesterol, and refined sugars (Appel *et al.,* 2011). The DASH diet provides essential micronutrients such as potassium, calcium, and magnesium, which contribute to vasodilation and decreased vascular resistance.

Furthermore, reducing sodium intake significantly lowers blood pressure by decreasing plasma volume and vascular reactivity. The World Health Organization recommends a daily sodium intake of less than 2 grams (5 grams of salt) per day (WHO, 2021). Studies show that reducing sodium intake can lower systolic blood pressure by 5–6 mmHg in hypertensive patients (Aburto *et al.,* 2013). In contrast, increasing dietary potassium—through foods like bananas, beans, and spinach—enhances sodium excretion and relaxes vascular smooth muscle, providing an additional reduction in blood pressure (Filippini *et al.,* 2020).

2. Weight Reduction

Obesity is a major modifiable risk factor for hypertension. Excess body weight increases cardiac output, sympathetic nervous system activity, and sodium retention, all of which elevate blood pressure (Hall *et al.,* 2015). Weight reduction has a direct and linear relationship with blood

pressure control; a decrease of approximately 1 mmHg in systolic blood pressure occurs for every kilogram of body weight lost (Neter *et al.,* 2003). Sustainable weight loss through caloric restriction and increased physical activity reduces the need for pharmacological therapy and lowers the risk of metabolic syndrome.

3. Physical Activity

Regular physical activity enhances cardiovascular fitness and endothelial function, both essential for blood pressure regulation. Aerobic exercises such as brisk walking, cycling, swimming, or jogging performed for at least 150 minutes per week can reduce systolic blood pressure by 4–9 mmHg (Cornelissen & Smart, 2013). Resistance training also contributes to improved arterial compliance and insulin sensitivity. Mechanistically, exercise induces vasodilation through increased nitric oxide production, decreased sympathetic tone, and improved baroreceptor sensitivity (Liu *et al.,* 2022).

4. Moderation of Alcohol Consumption

Excessive alcohol intake is strongly associated with hypertension. Alcohol raises blood pressure through mechanisms involving increased sympathetic activation, stimulation of the renin–angiotensin–aldosterone system (RAAS), and endothelial dysfunction (Roerecke *et al.,* 2017). The American Heart Association (AHA) recommends limiting alcohol to no more than two drinks per day for men and one drink per day for women. Reducing heavy drinking has been shown to decrease systolic blood pressure by up to 5 mmHg in heavy drinkers (Roerecke *et al.,* 2017).

5. Smoking Cessation

Although smoking does not directly cause sustained hypertension, it contributes significantly to vascular injury, oxidative stress, and endothelial dysfunction, which potentiate hypertensive complications (Primatesta *et al.,* 2001). Nicotine acutely increases blood pressure through catecholamine release and vasoconstriction. Smoking cessation improves arterial elasticity and reduces cardiovascular morbidity and mortality, making it a cornerstone of hypertension management (Virdis *et al.,* 2010).

6. Stress Reduction and Psychosocial Interventions

Psychological stress activates the sympathetic nervous system and hypothalamic-pituitary-adrenal (HPA) axis, resulting in elevated blood pressure. Stress management interventions including mindfulness-based stress reduction, yoga, deep breathing exercises, and cognitive-behavioral therapy have shown modest but clinically meaningful blood pressure reductions (Brook *et al.,* 2013). Regular sleep and maintaining social support networks also contribute to lower stress levels and improved cardiovascular outcomes (Spruill, 2010).

7. Limitation of Caffeine Intake

Caffeine causes transient increases in blood pressure by stimulating the central nervous system and blocking adenosine receptors. Although habitual coffee drinkers develop tolerance, hypertensive patients are advised to limit caffeine consumption to less than 300 mg per day, equivalent to about three cups of coffee (Mesas *et al.,* 2011).

1.4.9 Pharmacological Management of Hypertension

Antihypertensive agents are used to achieve and maintain optimal blood pressure, reduce cardiovascular risk, and prevent target organ damage. Their selection depends on patient comorbidities, age, and drug tolerance. Combination therapy may be required to attain target

blood pressure levels. The major drug classes include diuretics, angiotensin-converting enzyme (ACE) inhibitors, angiotensin II receptor blockers (ARBs), calcium channel blockers (CCBs), and beta-blockers, alpha blockers, direct vasodilators, centrally acting sympathomimetics.

1. Diuretics

Diuretics are among the earliest and most extensively studied antihypertensive agents, forming a cornerstone in the pharmacological management of hypertension. Their principal mechanism involves promoting renal excretion of sodium and water, thereby reducing extracellular fluid volume, cardiac output, and ultimately blood pressure. Over time, despite partial restoration of plasma volume, peripheral vascular resistance decreases, maintaining the antihypertensive effect (Whelton *et al.,* 2018).

Thiazide diuretics, such as hydrochlorothiazide and chlorthalidone, act mainly on the distal convoluted tubule where they inhibit the sodium-chloride symporter. This results in increased sodium and water excretion and mild potassium loss. The chronic antihypertensive effect of thiazides, however, extends beyond volume reduction to include a decrease in vascular smooth muscle resistance, likely through sodium depletion and altered intracellular calcium handling (Carey *et al.,* 2022). Loop diuretics, including furosemide and bumetanide, inhibit the sodium–potassium–chloride cotransporter in the thick ascending limb of the loop of Henle. This mechanism produces potent diuresis but relatively short-lived antihypertensive effects, making loop diuretics more suitable for patients with coexisting renal impairment or fluid overload rather than for long-term essential hypertension. Potassium-sparing diuretics, such as spironolactone, eplerenone, and amiloride, act on the collecting ducts. Spironolactone and eplerenone are aldosterone antagonists, preventing sodium reabsorption and potassium excretion, while

amiloride blocks epithelial sodium channels directly. These agents help conserve potassium and are especially beneficial in resistant hypertension or in patients with hyperaldosteronism.

Clinically, thiazide diuretics are considered first-line therapy for uncomplicated hypertension, particularly effective in older adults, individuals of African ancestry, and patients with salt-sensitive hypertension. Their efficacy, cost-effectiveness, and outcome benefits have been demonstrated in large-scale trials such as the The Antihypertensive and Lipid-Lowering Treatment to Prevent Heart Attack Trial (ALLHAT) study. Loop diuretics, although less favored for routine hypertension, play a critical role in conditions involving significant fluid retention, such as congestive heart failure or chronic kidney disease. Potassium-sparing diuretics serve as adjuncts to thiazides or loop diuretics to prevent hypokalemia and are key agents in resistant hypertension. Spironolactone, in particular, has shown added benefit in patients with primary aldosteronism and heart failure with reduced ejection fraction (Williams *et al.,* 2018).

Despite their efficacy, diuretics are associated with several adverse effects that necessitate careful monitoring. Thiazide diuretics may cause hypokalemia, hyponatremia, hyperuricemia leading to gout, and metabolic disturbances such as hyperglycemia and dyslipidemia. Loop diuretics can produce dehydration, electrolyte imbalance, metabolic alkalosis, and, at high doses, ototoxicity. Potassium-sparing diuretics, although protective against potassium loss, may cause hyperkalemia, especially when combined with renin–angiotensin system inhibitors. Spironolactone can lead to endocrine effects such as gynecomastia and menstrual irregularities due to its antiandrogenic properties. Electrolyte monitoring, therefore, remains crucial,

particularly in elderly or renally impaired patients (KDIGO, 2021).

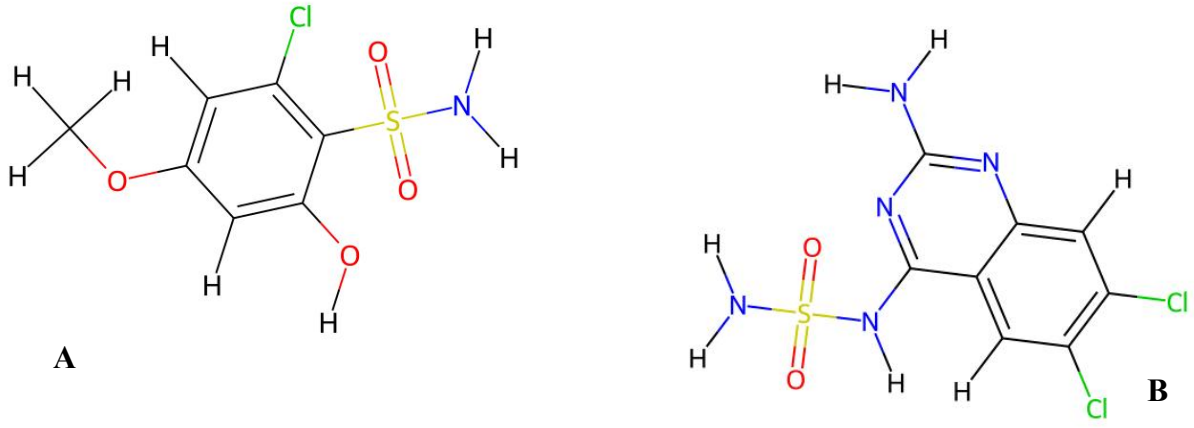

Figure 1.2 Structure of Furosemide (A) and Hydrochlorothiazide (B)

2. Beta Blockers

Beta-adrenergic blockers (commonly called beta blockers) are a class of drugs that antagonize the effects of catecholamines such as epinephrine and norepinephrine at β-adrenergic receptors. These agents play a significant role in cardiovascular medicine, including hypertension management, ischemic heart disease, arrhythmias, and heart failure. Although once considered first-line antihypertensive agents, current guidelines recommend their use primarily in patients with compelling cardiovascular comorbidities such as ischemic heart disease, heart failure, or post-myocardial infarction (Whelton *et al.,* 2018).

The mechanism of action of beta blockers involves blockade of β1-adrenergic receptors in the heart, leading to decreased heart rate (negative chronotropy), reduced myocardial contractility (negative inotropy), and diminished cardiac output. Additionally, inhibition of β1 receptors in the juxtaglomerular cells of the kidney reduces renin release, thereby attenuating the activation of the renin–angiotensin–aldosterone system (RAAS) and lowering systemic vascular resistance over time (Kjeldsen, 2018). Non-selective beta blockers, such as propranolol, block both β1 and

β2 receptors, whereas cardioselective agents like atenolol, metoprolol, and bisoprolol predominantly target β1 receptors, minimizing bronchoconstrictive effects associated with β2 inhibition. Third-generation beta blockers such as carvedilol and nebivolol possess additional vasodilatory properties mediated through α1 blockade or nitric oxide release, respectively, offering improved vascular and metabolic profiles (Messerli *et al.,* 2018).

From a clinical perspective, beta blockers are indicated in hypertensive patients with coexisting conditions including angina pectoris, arrhythmias, heart failure, and post-myocardial infarction syndromes, where they provide mortality and morbidity benefits. They are particularly valuable in patients with increased sympathetic drive or tachyarrhythmia. In younger patients and those with hyperkinetic circulation, beta blockers can effectively control elevated blood pressure and heart rate. However, as monotherapy in uncomplicated hypertension, their efficacy in preventing stroke and cardiovascular events has been shown to be inferior to that of other first-line agents such as thiazide diuretics or calcium channel blockers (Lindholm *et al.,* 2005).

Beta blockers can be broadly categorized into three generations based on receptor selectivity and additional pharmacologic properties. The first-generation (non-selective) agents—such as propranolol and nadolol—block both β1 and β2 receptors, affecting both cardiac and bronchial smooth muscle. The second-generation (cardioselective) agents—such as metoprolol, atenolol, and bisoprolol—primarily block β1 receptors at therapeutic doses, resulting in fewer respiratory side effects. The third-generation agents—carvedilol, labetalol, and nebivolol—combine β-blockade with vasodilatory actions either through α1 blockade or nitric oxide-mediated mechanisms, offering improved metabolic and hemodynamic profiles (Frishman, 2013).

Despite their therapeutic benefits, beta blockers are associated with several adverse effects that require careful monitoring. Common side effects include bradycardia, fatigue, exercise intolerance, and cold extremities. Non-selective agents may induce bronchospasm in asthmatic or chronic obstructive pulmonary disease (COPD) patients due to β2 blockade. They may also mask hypoglycemic symptoms in diabetic patients and contribute to metabolic disturbances such as insulin resistance and dyslipidemia. Sudden withdrawal can lead to rebound hypertension and tachycardia, highlighting the importance of gradual dose tapering. Carvedilol and nebivolol, due to their vasodilatory and antioxidative properties, tend to exhibit fewer metabolic adverse effects, making them more favorable in patients with metabolic syndrome (Bangalore *et al.,* 2007).

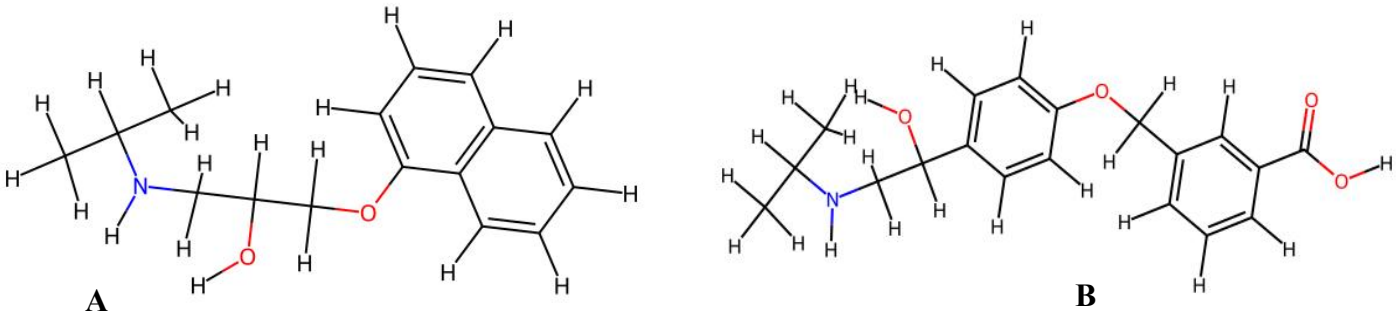

Figure 1.3 Structure of Propanolol (A) and Labetalol (B)

3. Calcium Channel Blockers

Calcium channel blockers (CCBs) are widely used in the management of hypertension, ischemic heart disease, and certain arrhythmias. Their antihypertensive action arises from inhibition of voltage-gated L-type calcium channels located in vascular smooth muscle and cardiac myocytes, leading to decreased intracellular calcium concentration, reduced vascular tone, and vasodilation (Pitt, 2018). These agents are particularly effective in reducing peripheral vascular resistance without significant effects on venous capacitance, thus lowering arterial blood pressure and afterload.

The mechanism of action of CCBs involves selective blockade of calcium influx through L-type calcium channels during membrane depolarization. This inhibition leads to relaxation of arterial smooth muscle, resulting in decreased systemic vascular resistance and arterial pressure. In the myocardium, CCBs reduce contractility, slow atrioventricular conduction, and decrease heart rate, these effects may vary depending on the subclass of CCB (Kjeldsen, 2018).

Calcium channel blockers are broadly classified into two major categories: dihydropyridines (DHPs) and non-dihydropyridines (non-DHPs).

Dihydropyridines, including agents such as amlodipine, felodipine, and nifedipine, primarily act on vascular smooth muscle to produce potent vasodilation with minimal direct cardiac effects. They are highly effective in lowering blood pressure, particularly in older adults and patients of African descent, where other agents such as beta blockers or ACE inhibitors may be less effective. Dihydropyridines are, therefore, recommended as first-line therapy for uncomplicated hypertension in many international guidelines (Williams *et al.,* 2018).

Non-dihydropyridines, such as verapamil and diltiazem, exert both vascular and cardiac effects. They decrease heart rate and myocardial contractility, making them particularly useful in patients with hypertension coexisting with supraventricular tachyarrhythmias or angina pectoris. However, their negative inotropic and chronotropic properties limit their use in patients with heart failure with reduced ejection fraction (Frishman, 2019).

From a clinical standpoint, CCBs offer several therapeutic advantages. They are effective as monotherapy or in combination with other antihypertensive agents, including ACE inhibitors, ARBs, or diuretics. The combination of a CCB with an ACE inhibitor is particularly effective and well tolerated, as it mitigates common side effects such as peripheral edema. CCBs have demonstrated significant efficacy in reducing cardiovascular events, stroke incidence, and overall mortality in hypertensive patients. For example, the ASCOT-BPLA and ALLHAT trials confirmed the benefit of amlodipine-based regimens in lowering stroke and coronary event rates compared to beta blocker–based therapies (Dahlöf *et al.,* 2005; ALLHAT, 2002).

Despite their proven efficacy, adverse effects may occur, varying by subclass. Dihydropyridines commonly cause vasodilatory side effects such as peripheral edema, flushing, headache, and reflex tachycardia. Extended-release formulations help reduce reflex sympathetic activation and improve tolerability. Non-dihydropyridines can cause bradycardia, atrioventricular block, and constipation (especially with verapamil). When used concomitantly with beta blockers, there is an increased risk of severe bradyarrhythmia or heart block, and thus this combination requires careful monitoring. Hepatic metabolism through the CYP3A4 enzyme system also poses potential for drug interactions (Messerli et al., 2018).

CCBs are particularly advantageous in special populations, including elderly patients, individuals of African ancestry, and those with isolated systolic hypertension, owing to their potent vasodilatory effect on large arteries. Additionally, they are beneficial in patients with angina, peripheral vascular disease, and metabolic syndrome, as they do not adversely affect lipid or glucose metabolism. Their use in pregnancy, however, requires caution, with nifedipine being the most commonly preferred agent when necessary.

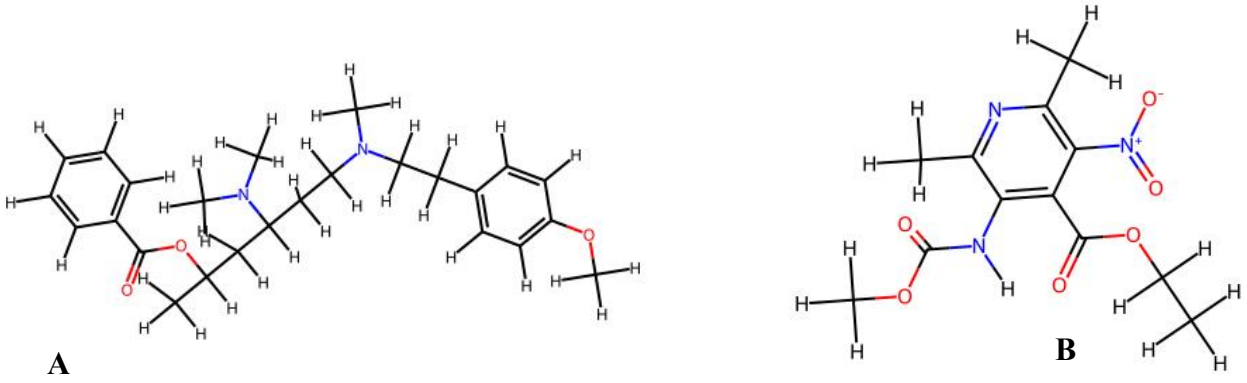

A **B**

Figure 1.4 Structure of Verapamil (A) and Nifedipine (B)

4. Alpha adrenergic Blockers

Alpha-adrenergic blockers (α-blockers) exert their effect by antagonizing post-synaptic α1-adrenergic receptors located on vascular smooth muscle. This blockade inhibits the binding of norepinephrine and epinephrine, resulting in vasodilation, decreased peripheral vascular resistance, and a subsequent reduction in blood pressure.

The mechanism of action of α-blockers centers on selective inhibition of α1-adrenergic receptors, leading to relaxation of arterial and venous smooth muscle. This effect reduces both systemic vascular resistance and venous return, thereby decreasing cardiac preload and afterload (Rang *et*

al., 2021). Unlike β-blockers, α-blockers do not significantly affect cardiac output, heart rate, or renin secretion. Additionally, they improve lipid metabolism by reducing total cholesterol and triglycerides while increasing high-density lipoprotein (HDL) cholesterol. The most commonly used selective α1-blockers include prazosin, doxazosin, and terazosin, while non-selective agents like phentolamine and phenoxybenzamine are reserved for conditions such as phaechromocytoma. In terms of clinical application, α-blockers are generally used as adjunctive therapy rather than first-line treatment for hypertension. They are particularly beneficial in patients with concomitant benign prostatic hyperplasia (BPH) due to their ability to relax smooth muscle in the bladder neck and prostate, thereby improving urinary flow. Doxazosin and terazosin are frequently employed in such dual indications (Kjeldsen, 2018). Additionally, α-blockers may be useful in patients with insulin resistance or dyslipidemia, as they do not adversely affect glucose metabolism and may improve lipid profiles. However, their long-term cardiovascular benefits remain uncertain.

Despite their therapeutic potential, adverse effects are an important limitation. Orthostatic hypotension is the most common and clinically significant side effect, especially after the first dose referred to as the "first-dose phenomenon." This can result in dizziness, syncope, or postural lightheadedness, particularly in elderly patients or those on diuretics. Slow titration and bedtime administration help minimize this risk. Other side effects include headache, nasal congestion, fatigue, and, less commonly, fluid retention and reflex tachycardia. Non-selective α-blockers such as phentolamine may provoke marked tachycardia due to unopposed β-adrenergic stimulation (Frishman, 2019).

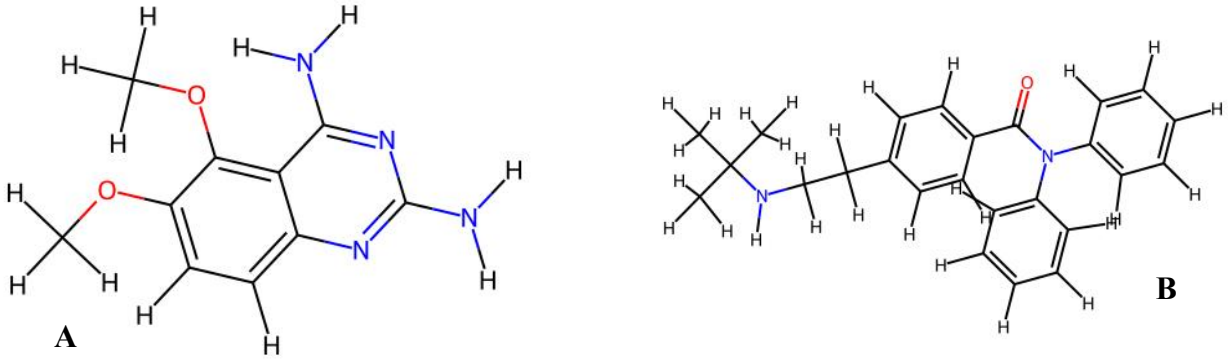

Figure 1.5 Structure of Prazosin (A) and Phentolamine (B)

5. Angiotensin-Converting Enzyme (ACE) Inhibitors and Angiotensin II Receptor Blockers (ARBs)

ACE inhibitors and ARBs are cornerstone agents in the pharmacological management of hypertension due to their proven efficacy in lowering blood pressure and reducing cardiovascular morbidity and mortality. Both drug classes act by interfering with the RAAS but at different molecular targets.

ACE inhibitors (e.g., enalapril, lisinopril, ramipril, captopril) inhibit the angiotensin-converting enzyme, which catalyzes the conversion of angiotensin I to angiotensin II, a potent vasoconstrictor. This inhibition decreases systemic vascular resistance and blood pressure while also reducing aldosterone secretion, leading to decreased sodium and water retention (Rang *et al.,* 2021). Additionally, ACE inhibitors prevent the breakdown of bradykinin, a vasodilatory peptide, further enhancing vasodilation but also contributing to side effects such as cough and angioedema.

ARBs (e.g., losartan, valsartan, candesartan, telmisartan) selectively block the binding of angiotensin II to the AT_1 receptor subtype on vascular smooth muscle and adrenal glands. This blockade prevents vasoconstriction and aldosterone release without affecting bradykinin metabolism, thus providing similar hemodynamic benefits with fewer adverse effects such as cough or angioedema (Carey *et al.,* 2018). ARBs, therefore, offer a more targeted RAAS inhibition while maintaining better tolerability.

Angiotensin-converting enzyme inhibitors (ACEIs) and angiotensin II receptor blockers (ARBs) are key agents in the treatment of hypertension, heart failure, diabetic nephropathy, and post-myocardial infarction remodeling (Whelton *et al.,* 2018). Both classes reduce vasoconstriction, aldosterone secretion, and improve cardiovascular outcomes. Adverse effects include cough and angioedema—more common with ACEIs due to bradykinin accumulation—hyperkalemia, hypotension, dizziness, and renal dysfunction (Messerli *et al.,* 2018). ARBs are often better tolerated.

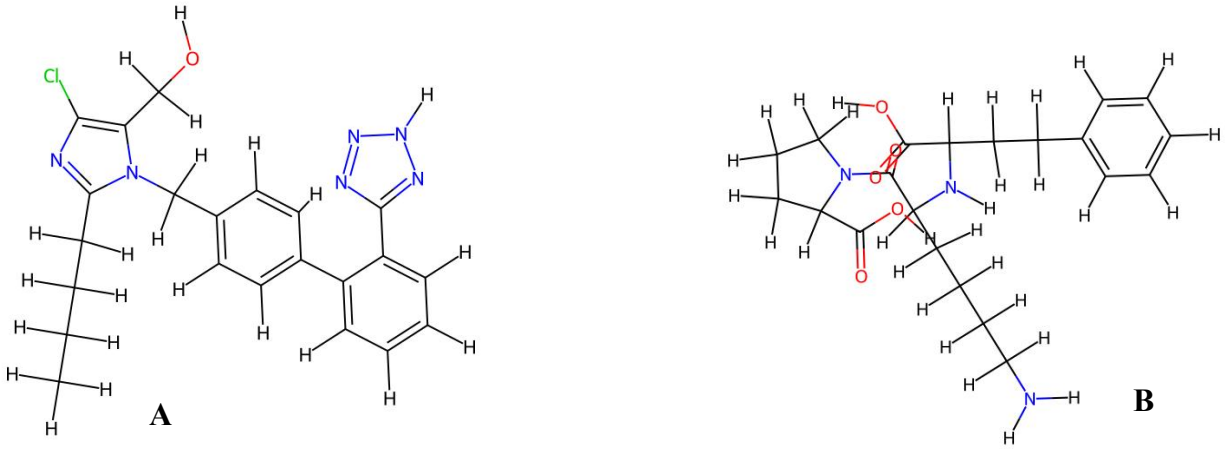

Figure 1.6 Structure of Losartan (A) and Lisinopril (B)

6. Vasodilators

Vasodilators lower arterial blood pressure by directly affecting vascular smooth muscle to decrease systemic vascular resistance. Unlike many antihypertensive agents that modulate neurohormonal systems, direct vasodilators exert their effect primarily via relaxation of arterial (and in some cases venous) smooth muscle. They are typically reserved for specific clinical situations, such as resistant hypertension or hypertensive emergencies, pregnancy-related hypertension because their use is often limited by compensatory mechanistic responses and adverse effects.

Direct vasodilators reduce blood pressure through arteriolar dilation, which lowers systemic vascular resistance (SVR). In the case of hydralazine, the drug preferentially dilates resistance (arteriolar) vessels, decreasing afterload; venous capacitance vessels are less affected, which somewhat lessens orthostatic hypotension. Minoxidil works by opening ATP-sensitive potassium channels in vascular smooth muscle, causing hyperpolarization and vasodilation primarily of arterioles rather than veins. These reflex responses limit their standalone use and require concomitant therapy such as a diuretic and a β-blocker. (Cohn, *et al.,* 2011).

Vasodilators may cause reflex tachycardia, fluid retention, headache, and flushing due to compensatory sympathetic activation. Hydralazine can induce a lupus-like syndrome, while minoxidil may cause hypertrichosis and pericardial effusion. Hypotension and palpitations are common, necessitating concurrent use of β-blockers and diuretics to minimize adverse cardiovascular and renal effects (ESH, 2023).

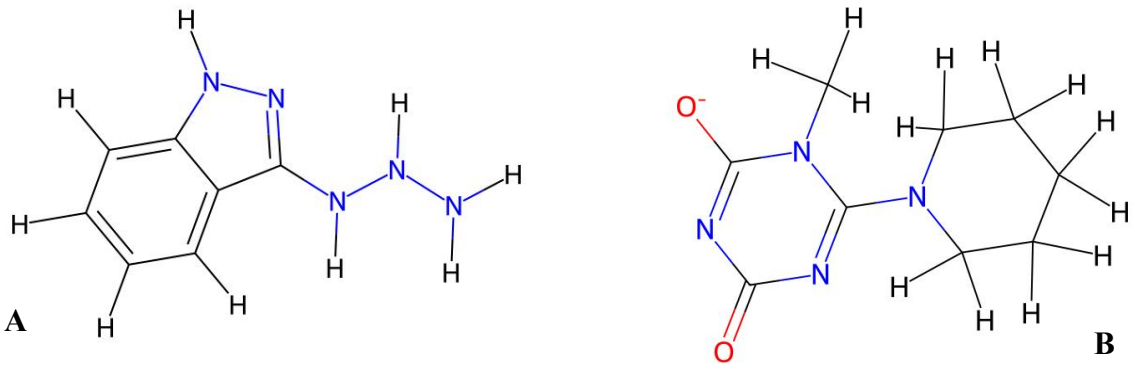

Figure 1.7 Structure of Hydralazine (A) and Minoxidil (B)

7.

Centrally Acting Sympatholytics

Centrally acting sympatholytic (or sympathomimetic-modulating) antihypertensive agents exert their effect primarily by reducing sympathetic nervous system outflow from the brainstem rather than acting peripherally. They stimulate central α_2-adrenergic receptors and/or imidazoline I_1-receptors in regions such as the rostral ventrolateral medulla, thus decreasing norepinephrine release, reducing total peripheral resistance, heart rate, and cardiac output. (Schlaich *et al.,* 2020).

Historically, agents such as Clonidine and Methyldopa (acting mainly via α_2-agonism) were used widely; later agents like Moxonidine and Rilmenidine are more selective for imidazoline I_1-receptors, which offers improved tolerability (fewer sedative or dry-mouth effects).(Schlaich *et al.,* 2024)

In major hypertension guidelines, centrally acting sympatholytic drugs are not first-line agents; rather, they are listed among the second- or later-line add-on therapies. Adverse effects remain a major limitation: common issues include fatigue, sedation, dry mouth, constipation, bradycardia, orthostatic hypotension and on abrupt withdrawal rebound hypertension due to sudden

sympathetic surge. Therefore, when used gradual tapering is essential if discontinuation is planned. Clinically, they may be considered in patients with difficult-to-control hypertension, especially when other classes have been optimized, provided the side-effect profile is acceptable. (Whelton *et al.,* 2018; Carey *et al.,* 2018)

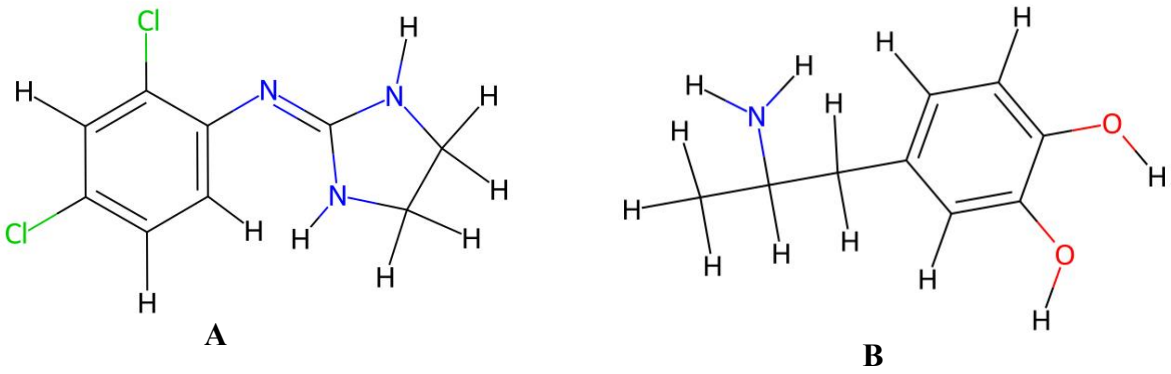

Figure 1.8 Structure of Clonidine (A) and Methyldopa (B)

1.5 Imidazole

The imidazole ring is a planar five-membered aromatic heterocycle composed of three carbon atoms and two nitrogen atoms located at the 1- and 3-positions. Its structure allows for tautomerism, hydrogen-bonding capacity, and coordination with metals (Parmar *et al.,* 2024; Abdallah *et al.,* 2024). Imidazole occurs naturally in many biological molecules. It forms the core of the amino acid histidine and its decarboxylation product histamine, essential in enzyme catalysis and immune response. Imidazole rings are also present in purine nucleotides such as adenine and guanine, contributing to DNA and RNA structure. Additionally, it appears in vitamins like biotin and various natural alkaloids, highlighting its widespread biological significance in diverse living organisms, across cellular metabolism (De Luca & Giacomelli,

2006). Because of its presence in endogenous molecule, imidazole is considered a bio-relevant structure.

Imidazoline is a partially saturated analogue of imidazole, containing a single double bond within the ring. The structural change alters the molecule's electronic distribution and binding characteristics, allowing selective interaction with specific receptor subtypes. Imidazoline derivatives contain the –C(=NH)–NH– functional group and can form hydrogen bonds with receptor sites involved in cardiovascular control.

1.5.1 Bioactivity of Imidazole

Imidazole and imidazoline derivatives possess wide therapeutic applications due to their diverse pharmacological properties.

1. Antifungal Activity

Imidazole derivatives are widely used as antifungal agents by inhibiting ergosterol synthesis, an essential component of fungal cell membranes. Drugs such as clotrimazole and miconazole disrupt membrane integrity, leading to fungal cell death. Clinically, imidazole antifungals are used to treat candidiasis, dermatophytosis, and Aspergillus infections. Their broad activity and good topical tolerance make them first-line therapy in many superficial fungal infections (Pappas *et al.,* 2016).

2. Antimicrobial Activity

Imidazole compounds display broad antibacterial activity by interfering with microbial protein synthesis and membrane stability. Their structural versatility allows interaction with enzymes essential for bacterial survival. While not the primary choice against all bacterial infections, imidazole derivatives like metronidazole are clinically vital for treating anaerobic bacterial and protozoal diseases such as bacterial vaginosis, amoebiasis, and giardiasis (Brook, 2016).

3. Anticancer Activity

Imidazole-containing compounds exhibit anticancer potential through DNA binding, inhibition of cell proliferation, and disruption of tumor metabolism. Some derivatives target kinase-mediated growth pathways, inducing apoptosis in cancer cells. Clinical research has led to imidazole-based drugs like dacarbazine used in melanoma and Hodgkin's lymphoma therapy. Their selectivity and ability to interfere with tumor cell replication make them valuable chemotherapeutic agents (Zhou *et al.,* 2017).

4. Anti -inflammatory and Analgesic Activity

Imidazole derivatives reduce inflammation by modulating cyclooxygenase (COX) pathways and inhibiting pro-inflammatory cytokines. Some compounds suppress oxidative stress and leukocyte activation, contributing to decreased tissue damage. Though not as commonly prescribed as NSAIDs, imidazole-based molecules remain promising candidates in drug development for chronic inflammatory disorders, including arthritis and airway inflammation (Awasthi *et al.,* 2013).

5. Antihypertensive Activity

Certain imidazole derivatives act on imidazoline receptors, influencing sympathetic nervous system activity and lowering blood pressure. For example, clonidine and moxonidine reduce peripheral vascular resistance by decreasing central adrenergic outflow. Clinically, these drugs are indicated in the management of hypertension, especially in patients unresponsive to standard therapies. Their utility lies in long-term regulation of blood pressure and reduction of catecholamine-mediated vasoconstriction (Schlaich *et al.,* 2024).

6. Anti-ulcer Properties

Imidazole-containing compounds are well-recognized for their anti-ulcer activity, primarily through their role as H2 receptor antagonists, which inhibit gastric acid secretion. Drugs such as Cimetidine, Ranitidine, Famotidine, and Nizatidine possess the imidazole moiety, enabling selective binding to H2 receptors in the stomach lining and thereby reducing gastric acidity. This structural feature contributes not only to effective ulcer healing but also to cytoprotection of the gastric mucosa, highlighting the therapeutic relevance of the imidazole in peptic ulcer management.

1.5.2 Chemistry of Imidazole

1.4.2.1 Physiochemical Properties of Imidazole

The presence of two nitrogen atoms at non-adjacent positions, gives imidazole its amphoteric characteristics, this duality allows imidazole to participate in a variety of reactions. It also exhibits high polarity, moderate water solubility, and a melting point of approximately 90–91 °C. The nitrogen at position 3 contributes to basicity (pKa ~7), allowing imidazole to act as a proton donor or acceptor, making it versatile in hydrogen bonding. Its aromaticity stabilizes the ring, while the lone pair electrons on nitrogen enable metal coordination and enzymatic interactions

(Parmar *et al.,* 2024; Abdallah *et al.,* 2024).The presence of basic imidazole nitrogen also allows salt formation and exhibits high polarity and strong hydrogen-bonding capacity, which may improve aqueous solubility.

Structure-Activity Relationship (SAR) studies of imidazole derivatives indicate that substitution at N-positions can modulate lipophilicity and metabolic stability; substitution at C-positions often influences binding affinity to biological targets. For instance, electron-withdrawing substituents at the C-2 position increase potency in antimicrobial assays, while bulky aryl substituents at C-4/5 enhance receptor binding in anticancer models (Mumtaz *et al.,* 2023).

1.5.5 Chemical Synthesis of Imidazole

Imidazole can be synthesized through a variety of chemical routes, broadly classified into several major types based on the precursors and reaction conditions. These methods allow the construction of the five-membered heterocyclic ring with diverse substitution patterns, which is essential in drug development. The principal synthetic approaches include:

1. Debus–Radziszewski Synthesis:

One of the most common methods, it involves the condensation of a 1,2-dicarbonyl compound, an aldehyde, and ammonia or an amine to form the imidazole ring. This method is versatile, allowing the introduction of substituents at C2, C4, and C5 positions.

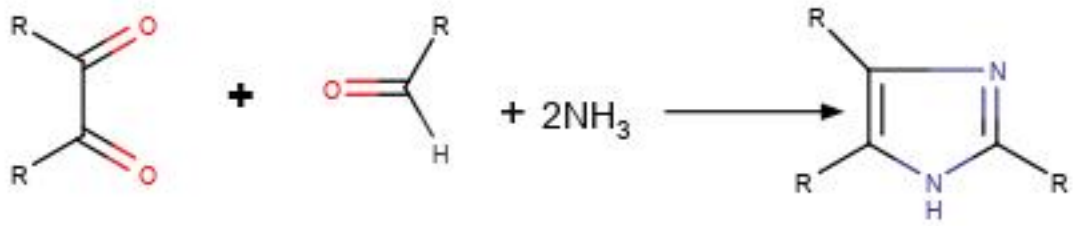

Figure1.10: Reaction scheme showing debus–radziszewski synthetic pathway

2. Markwald Synthesis of Imidazole

This is a classical method for preparing 2-substituted imidazoles, particularly 2-mercaptoimidazoles. In this reaction, α-amino ketones or α-amino aldehydes react with potassium thiocyanate or alkyl isothiocyanates to form the corresponding 2-mercaptoimidazole derivatives. The sulfur atom in the 2-mercaptoimidazole can then be removed using various oxidative methods to yield the desired imidazole (Rama Brahma Reddy *et al.,* 2022).

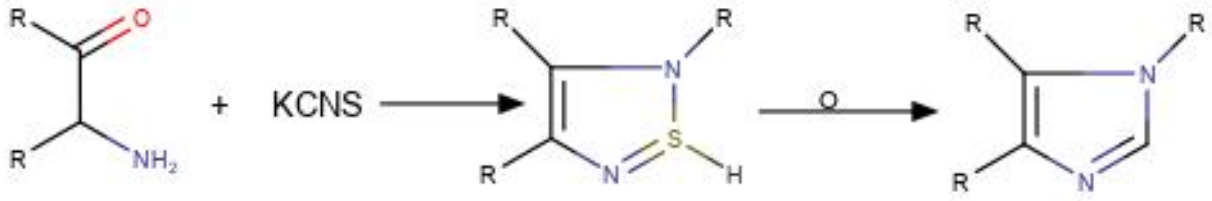

Figure 1.11: Reaction scheme showing markwald synthetic pathway

3. Synthesis of Imidazoles from α-Haloketones

Imidazoles can be efficiently synthesized through the reaction of amidine or imidine derivatives with α-haloketones. This approach allows the formation of substituted imidazoles, including 2,4- or 2,5-biphenyl imidazoles. For example, the condensation of phenacyl bromide with benzimidine under appropriate conditions affords 2,4-diphenyl imidazole. Similarly, amidines

can react with acyloins or α-haloketones to yield imidazole rings, providing a versatile pathway for introducing substituents at the 2- and 4-positions(Rama Brahma Reddy *et al.,* 2022).

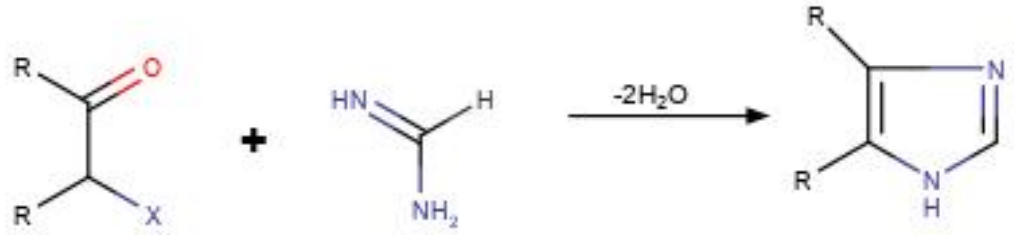

Figure 1.12: Reaction scheme showing imidazole synthesis from α-haloketones

1.6 Imidazoline Receptors

The concept of imidazoline receptors emerged in the late 20th century following observations that certain imidazoline-containing compounds, such as clonidine, exhibited physiological effects that could not be fully explained by their known interactions with α_2-adrenergic receptors. Subsequent research led to the identification of non-adrenergic binding sites that displayed high affinity for imidazoline derivatives but low affinity for catecholamines. These distinct sites were termed imidazoline receptors, now recognized as an independent receptor system with diverse physiological roles in cardiovascular, renal, and metabolic regulation (Head & Mayorov, 2021).

Structurally, imidazoline receptors are membrane-associated proteins that bind selectively to ligands containing an imidazoline or imidazolidine nucleus. Although their exact molecular identity remains incompletely defined, several candidate proteins have been proposed. These receptors exhibit unique binding characteristics, distinct from G protein-coupled α-adrenergic receptors, suggesting they belong to a separate receptor superfamily. Their binding affinity for imidazoline ligands depends on the presence of the planar imidazoline ring, which interacts with specific polar and hydrophobic residues within the receptor's active site (Piletz *et al.,* 2013).

Imidazoline receptors are generally classified into three subtypes: I_1, I_2, and I_3 receptors, based on their tissue distribution, ligand selectivity, and functional properties.

The I_1 subtype is primarily located in the rostral ventrolateral medulla (RVLM) of the brainstem, where it plays a critical role in modulating sympathetic outflow and baroreceptor reflex sensitivity. I_1 sites have also been identified in peripheral tissues, including the kidney, pancreas, and liver, indicating broader physiological functions. The I_2 subtype is localized predominantly in mitochondrial membranes and is associated with monoamine oxidase (MAO) enzymes. Unlike I_1, I_2 receptors are implicated in modulating oxidative metabolism and neurochemical processes. The I_3 subtype, although less well characterized, is expressed in pancreatic β-cells and may influence insulin secretion, indicating a potential link between imidazoline signaling and glucose homeostasis (Molderings *et al.,* 2019).

Activation of I_1 receptors triggers multiple downstream pathways, including modulation of phosphatidylcholine-specific phospholipase C and regulation of protein kinase C activity, which in turn influence neuronal excitability and vascular tone (Ernsberger, 2020). I_2 receptors, on the other hand, are thought to exist as allosteric sites on MAO-A or MAO-B or as distinct mitochondrial proteins. Their interaction with imidazoline ligands alters mitochondrial function and energy metabolism, suggesting a role in cellular redox regulation. The I_3 subtype remains the least understood but is hypothesized to interact with ATP-sensitive potassium channels, influencing pancreatic β-cell depolarization and insulin release. Hence midazoline receptors represent a unique class of binding sites that interact specifically with imidazoline-based ligands through distinct structural and biochemical mechanisms.

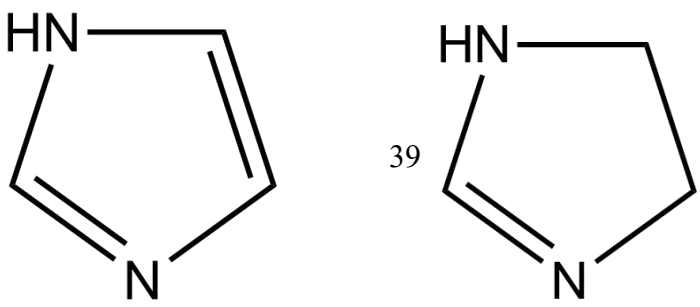

A **B**

Figure 1.12 Structure of Imidazole (A) and Imidazoline (B)

1.7 Justification of Study

Hypertension remains a silent killer responsible for millions of deaths annually and poses a significant health challenge in low- and middle-income countries like Nigeria. Despite the availability of several antihypertensive drugs, many patients still experience poor blood pressure control, adverse drug reactions, and therapeutic resistance. This highlights the urgent need for novel antihypertensive agents with improved efficacy and safety profiles. Imidazole and its derivatives have gained significant attention in medicinal chemistry due to their diverse biological activities, including antihypertensive, anti-inflammatory, and antioxidant properties. Their structural versatility allows for molecular modifications that can enhance receptor binding and pharmacodynamic effects on vascular targets such as the angiotensin II receptor or imidazoline receptors. Employing in silico screening facilitates the rapid identification of potent imidazole-based compounds with favorable pharmacokinetic and toxicity profiles before laboratory synthesis, thus saving time and resources. Subsequent synthesis and characterization confirm molecular identity and purity, ensuring reproducibility and reliability of results. This study, therefore integrates computational modeling and experimental techniques to design a series of imidazole derivatives, synthesize, and evaluate an imidazole derivative with potential antihypertensive activity, contributing to the ongoing search for safer and more effective therapies for hypertension management.

1.8 Aim and Objective of Study

The aim of this study is to identify and evaluate some imidazole-based compounds with potential antihypertensive activity through a combination of computational and laboratory approaches. The research will involve in silico screening to predict binding affinity and pharmacokinetic properties, followed by chemical synthesis of a selected lead compound. The synthesized derivative will be subjected to structural characterization using analytical techniques to confirm its identity and purity. The findings of this work are intended to support the rational design of novel therapeutic compounds capable of improving current hypertension management.

1.9 Specific Objectives

- To rationally design and model imidazole derivatives for potential to antihypertensive activity
- To perform molecular docking and binding energy analysis of the designed derivatives against hypertension targets.
- To assess ADME and toxicity profiles of the screened derivatives using in silico predictive tools.
- To synthesize the lead imidazole derivative identified from computational screening.
- To characterize the synthesized compound(s) using analytical techniques to confirm identity and purity.

CHAPTER TWO

MATERIALS AND METHODS

2.1 Materials

2.1 Software and Computational Tools

1. RCSB PDB

The Research Collaboratory for Structural Bioinformatics Protein Data Bank (RCSB PDB) is an essential bioinformatics resource for retrieving three-dimensional structures of biological macromolecules, including enzymes and receptors relevant to drug design. The database allows researchers to visualize molecular conformations, analyze binding interactions, and perform computational modeling. It provides experimentally validated structures determined by X-ray crystallography, NMR spectroscopy, or cryo-electron microscopy. In in-silico studies, such as molecular docking, the RCSB PDB serves as the primary source for target proteins, allowing researchers to explore ligand–protein interactions and identify potential drug-binding sites. Thus, it plays a crucial role in structure-based drug discovery. (Rose *et al.,* 2017; Burley *et al.,* 2021)

2. PubChem Database

The PubChem database, maintained by the National Center for Biotechnology Information (NCBI), is a comprehensive public repository for chemical information, including molecular structures, properties, bioactivities, and pharmacological data. It integrates information from multiple sources to support cheminformatics, drug discovery, and virtual screening studies. Researchers use PubChem to obtain ligand structures for molecular docking, predict biological activities, and analyze structure–activity relationships. Its interactive tools enable the visualization and comparison of compounds relevant to specific biological targets, such as

antihypertensive agents. PubChem thus plays a pivotal role in computational drug design and pharmacological research (Kim *et al.,* 2016; Kim *et al.,* 2023).

3. Discovery studio 2020 client

An advanced computational chemistry and molecular modeling software widely used in structure-based drug design and bioinformatics research. It provides an interactive environment for visualizing, simulating, and analyzing biomolecular structures, protein–ligand interactions, and pharmacophore models. The software integrates tools for molecular docking, dynamics, QSAR studies, and ADMET prediction, facilitating the identification and optimization of potential drug candidates.

4. PyRx Software

PyRx is an open-source virtual screening tool that integrates computational docking and molecular modeling functionalities. It simplifies the process of ligand preparation, energy minimization, and docking using AutoDock Vina or AutoDock 4. PyRx provides an intuitive graphical interface for screening multiple compounds against biological targets, making it valuable for structure-based drug discovery and lead optimization (Dallakyan & Olson, 2015).

5. PyMOL

PyMOL is a powerful molecular visualization and modeling program widely used in structural biology, bioinformatics, and computational drug discovery. It provides detailed three-dimensional representations of proteins, nucleic acids, and small molecules, allowing users to explore binding sites, measure molecular distances, and create high-quality graphical images. In in-silico studies, PyMOL is instrumental for analyzing molecular docking results, visualizing

protein–ligand interactions, and examining conformational dynamics. Its Python-based scripting environment enhances reproducibility and data analysis, making it an essential tool in modern structure-based drug design and discovery.

6. Marvin Sketch

A chemical drawing and visualization software that allows researchers to design, edit, and analyze chemical structures with high precision. It supports the drawing of organic, inorganic, and macromolecular compounds and can automatically generate chemical names, molecular formulas, and physicochemical properties. MarvinSketch integrates predictive tools for pKa, logP, and other molecular descriptors, making it highly useful in medicinal chemistry and computational drug design. In in-silico studies, it aids in preparing ligand structures for docking and virtual screening, ensuring accurate molecular geometry and annotation

7. SwissADME

SwissADME is a freely accessible web-based tool for evaluating the pharmacokinetic and physicochemical properties of small molecules. It predicts key parameters related to Absorption, Distribution, Metabolism, and Excretion (ADME), along with drug-likeness, bioavailability, and molecular descriptors. Researchers use SwissADME to assess compliance with Lipinski's Rule of Five, identify potential pharmacokinetic liabilities, and visualize the BOILED-Egg model for passive absorption and brain penetration. Its predictive reliability and integration of multiple computational models make it an essential tool in virtual screening and rational drug design(Daina, *et al.,* 2017)

8. ProTox 3.0

Developed to aid drug discovery and safety assessment, ProTox predicts various toxicity endpoints, including acute toxicity, hepatotoxicity, cytotoxicity, mutagenicity, and carcinogenicity. The tool integrates molecular fingerprints and toxicophore-based approaches to estimate LD_{50} values and assign compounds to toxicity classes according to Organisation for Economic Co-operation and Development (OECD) guidelines. Researchers use ProTox-3.0 to screen drug candidates for potential toxic effects prior to synthesis, thereby reducing laboratory costs and ethical concerns associated with animal testing.

2.1.2 Chemicals and Reagents

Benzil (Energy Chemistry®), Ammonium acetate (Nanjing Duly), Benzaldehyde (Macklin®) Absolute ethanol (GHTECH), ethyl acetate (Molychem®), glacial acetic acid (Molychem®), silica gel (Loba Chemie®), dichloromethane (Molychem®), n-hexane (Molychem®) and deionized water

2.1.3 Equipment and Materials

Three neck round bottom flask, test tubes and racks, capillary tubes, conical flasks, beakers, reflux condenser, sample bottles, chromatographic column, thin layer chromatographic plates, label, glass stirrer, mercury thermometer, pipette, filter papers, retort stand, thermometer, spatula, foil paper, analytical weighing balance, magnetic stirrer and heater, ultraviolet lamp.

2.2 Method

2.2.1 Target Protein Selection and Preparation

The three-dimensional crystal structures of the target proteins were obtained from the Research Collaboratory for Structural Bioinformatics Protein Data Bank (RCSB PDB) (Burley *et al.,* 2023). The structure corresponding to PDB ID 1O86 was located by searching the RCSB PDB database (https://www.rcsb.org) using its unique identifier. After identification, the structure file was downloaded in PDB format and saved for analysis. The downloaded protein structure was then imported into BIOVIA Discovery Studio for visualization and preparation. This was carried out by launching the software, navigating to the stored file via the 'File' menu, and selecting the import molecule option to load the structure into the workspace for further computational processing which included the addition of hydrogen ion and any non-protein atoms that were not pertinent to the investigation, such as ligands or water molecules, were eliminated in order to prepare the protein structure for additional research. Ultimately, the finalized protein structure was stored in Discovery Studio in an appropriate file format, like PDB or MOL2. The completed construction was kept in a predetermined spot in case it was needed for upcoming docking simulations or more research. This same procedure was followed in downloading and preparation of subsequent proteins with PDB ID; 4ZUD, 5XPR, and 6L88.

A B

Figure 2.1 Cryo-EM structure of the protein targets; 1O86(A) and 4ZUD(B).

A B

Figure 2.2: Cryo-EM structure of the protein targets; 5XPR(A) and 6L88(B).

2.2.2 Preparation of Ligands

The chemical structures of selected imidazole-based compounds were retrieved from the PubChem database in SDF format (Kim *et al.,* 2023). These parent structures were then modified using MarvinSketch to generate novel analogs through structural editing and substitution

reactions (ChemAxon, 2021). The resulting compounds were imported into PyRx for virtual screening, utilizing the Open Babel module to optimize geometry and convert the molecular structures into PDBQT format for docking simulations (Dallakyan and Olson, 2015; O'Boyle *et al.,* 2011). The ligands were energy-minimized prior to docking to ensure proper conformational stability for accurate binding assessments.

2.2.3 Protein- Ligand docking

The prepared protein structure was loaded into PyRx, where the AutoDock tool was used to convert the structure into a macromolecule format and visualize the potential binding pockets. Ligand structures and standard reference compounds in SDF format were imported using the Open Babel plugin, which converted them into PDBQT format following energy minimization to ensure stable conformers (O'Boyle *et al.,* 2011; Dallakyan and Olson, 2015). Molecular docking simulations were then performed using AutoDock Vina within the PyRx environment to evaluate the interaction of the imidazole derivatives with the target protein structures, specifically PDB IDs 1O86, 4ZUD, 5XPR and 6L88 (Trott and Olson, 2009). Grid box dimensions were defined based on previously reported key active site residues identified from the PyMOL to ensure precise binding site targeting (Samarakoon *et al.,* 2023).

2.2.4 Post Docking Analysis

A. Protein-ligand complex pharmacophores modelling

Following completion of the docking, the preferred docking conformations for each ligand were exported from PyRx in PDB format and Subsequent interaction analysis was performed using BIOVIA Discovery Studio Visualizer 2020, where both 2D and 3D interaction profiles were generated to examine the orientation of ligands within the active binding pocket. Special

attention was given to hydrogen bonding, hydrophobic contacts, and interactions with key amino acid residues, allowing identification of ligands with greater potential for effective receptor modulation and possible antihypertensive activity (Laskowski and Swindells, 2011).

B. ADMET Properties (Absorption, Distribution, Metabolism, Excretion and Toxicity)

The pharmacokinetic and safety profiles of the test compounds were evaluad in silico using the SwissADME web server, which provides integrative computational models for predicting ADMET characteristics (Daina *et al.,* 2017). Key parameters assessed included drug-likeness, pharmacokinetics, toxicity, water solubility (Log S), lipophilicity (Log P), and bioavailability scores. Lipophilicity was estimated using multiple algorithms XLOGP3, WLOGP, MLOGP, iLOGP, and SILICOS-IT with the consensus Log P calculated as the mean of values across these models, allowing for improved prediction reliability (Daina *et al.,* 2017).

Water solubility (Log S) predictions were derived from the SILICOS-IT model, while Lipinski's Rule of Five was applied to assess drug-likeness and oral bioavailability suitability. Predicted pharmacokinetic behaviors included skin permeability, gastrointestinal (GI) absorption, blood–brain barrier (BBB) penetrability, and potential interaction with major metabolic transport systems such as cytochrome P450 (CYP) enzymes and P-glycoprotein (P-gp) efflux transporters, as these factors influence systemic distribution and clearance (Daina *et al.,* 2017).

C. Toxicity Profile Determination

The ProTox-3.0 web server was employed to predict the toxicity profiles of the selected imidazole-based ligands. The chemical structures of the ligands were input either directly as SMILES notations or uploaded from structural files. The platform generated computational predictions for multiple toxicity endpoints, including respiratory toxicity, neurotoxicity,

nephrotoxicity, mutagenicity, and carcinogenicity. The resulting outputs were reviewed alongside the confidence probability scores provided by ProTox-3.0 to assess the reliability of each prediction and to guide interpretation of potential toxicity risks.

2.2.5 Synthesis of 2,4,5- Triphenyl-1H-Imidazole

The synthesis of the imidazole derivative was performed using the Debus–Radziszewski imidazole synthesis method, which involves the condensation of a 1,2-dicarbonyl compound, an aldehyde, and an amine source under controlled reaction conditions to form the imidazole ring.

Scheme of Reaction

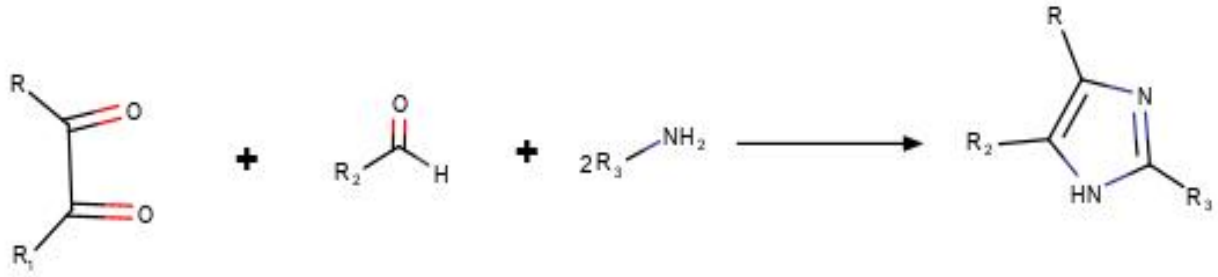

Figure 2.3: Imidazole scheme of reaction

2.2.5.1 Synthesis of 2,4,5-Triphenyl-1H-Imidazole

2.65 g of benzil and 5 g of ammonium acetate were placed into a three-neck round-bottom flask and dissolved in 31.25 mL of glacial acetic acid. The reaction mixture was stirred and maintained under reflux at temperature of 80-100^{0}C for 1 hour. Separately, 1.26 mL of benzaldehyde was dissolved in 6.25 mL of glacial acetic acid and introduced dropwise into the reaction mixture over 15–20 minutes, while maintaining the same reaction temperature. The mixture was then stirred under reflux for an additional 4 hours. (Jain *et al*., 2010)

Reaction progress was monitored using thin-layer chromatography (TLC) with n-hexane:ethyl acetate as the mobile phase. After completion, the mixture was allowed to stand overnight before filtration to remove any insoluble materials. The filtrate was then treated with 150 mL of cold deionized water, leading to the formation of a precipitate. The solid was collected by filtration, dried, and recrystallized from ethanol to obtain the purified product.

The obtained reaction product was further purified using column chromatography. Silica gel served as the stationary phase, while a solvent system composed of n-hexane, dichloromethane, and ethyl acetate in the ratio of 10:10:1 was employed as the mobile phase. Fractions were collected and monitored, after which the fraction containing the target compound was concentrated and dried to yield the purified imidazole derivative.

2.2.6 Melting Point Determination

The melting point of the synthesized 2,4,5-triphenyl-1H- imidazole compound was determined using a standard capillary melting point apparatus. A capillary tube was sealed at one end using a Bunsen burner, and a small quantity of the dried compound was introduced into the tube. The loaded capillary tube was then placed in the melting point apparatus. The temperature was increased gradually, and the temperatures corresponding to the onset of melting and the point at which the compound completely liquefied were recorded. This procedure followed the conventional capillary method for melting point determination, which is commonly employed to assess compound purity.

CHAPTER THREE

RESULTS

3.1: Binding Affinities

The active site residues of the selected protein targets (PDB IDs: 1O86, 4ZUD, 5XPR and 6L88), as identified using PyMOL, are presented in Tables 3.1, 3.2, 3.3, and 3.4 respectively.

The binding affinities of the synthesized imidazole derivatives and the reference ligand for the protein targets (1O86, 4ZUD, and 6L88) are shown in Tables 3.5, 3.6, 3.7, and 3.8 respectively.

Table 3.1: Amino acid binding sites of protein 1O86 identified with PyMOL

S/N	Amino acid binding sites
1	GLU 162
2	GLN 281
3	HIS 353
4	ALA 354
5	SER 355
6	ASP 377
7	VAL 379
8	VAL 380
9	HIS 383
10	GLU 384
11	HIS 387
12	ASP 415
13	ASP453
14	LYS 454
15	PHE457
16	LYS511
17	PHE512
18	HIS 513
19	TYR 520
20	TYR 521
21	TYR 523
22	PHE 527

Table 3.2: Amino acid binding sites of protein 4ZUD identified with PyMOL

S/N	Amino acid binding sites
1	TYR 35
2	PHE 77
3	TRP 84
4	TRP 87
5	THR 88
6	TYR 92
7	SER 105
8	VAL 108
9	SER 109
10	LEU 112
11	ALA 163
12	ARG 167
13	PHE 182
14	LYS 199
15	PRO 285
16	ILE 288
17	TYR 292

Table 3.3: Amino acid binding sites of protein 4ZUD identified with PyMOL

S/N	Amino acid binding sites
1	HIS 150
2	ASP 154
3	ASN 158
4	LYS 161
5	TRP 167
6	CYS 174
7	VAL 177
8	PRO 178
9	GLN 181
10	LYS 182
11	VAL 185
12	GLU 236
13	PHE 240
14	CYS 255
15	LYS 272
16	LEU 277
17	TYR 281
18	TRP 336
19	LEU 339
20	HIS 340
21	ARG 343
22	ILE 372
23	ALA 375

Table 3.4: Amino acid binding sites of protein 6L88 identified with PyMOL

S/N	Amino acid binding sites
1	ASN 770
2	LEU 772
3	ALA 773
4	LEU 766
5	LEU 769
6	GLN 776
7	VAL 780
8	TRP 806
9	MET 807
10	LEU 809
11	SER 810
12	ALA 813
13	ARG 817
14	MET 845
15	MET 852
16	TYR 869
17	LYS 873
18	CYS 942

KEY:

PHE- Phenylalanine

LEU: Leucine

GLU: Glutamic acid

ALA: Alanine

MET: Methionine

ILU: Isoleucine

TYR: Tyrosine

ARG: Arginine

TRP: Tryptophan

CYS: Cysteine

GLN: Glutamine

ASN: Asparagine

VAL: Valine

PRO: Proline

Table 3.5: Binding affinities of imidazole derivatives with 1O86

Compounds	CID	ΔG (Kcal/mol)	Energy
1-benzoyl-2-hexyl-4-methoxy-5-methyl-1H-imidazole	560912	-7.3	
2-(2-methoxyphenyl)-4,5-diphenyl-1H-imidazole	74782	-9.7	
1-benzoyl-2-hexyl-4,5-diphenyl-1H-imidazole	110237	-8.8	
2,4,5-triphenyl-1H-imidazole	10232	-9.4	
2-amino-1-benzoyl-1H-1,3-benzodiazole-5-carboxamide	642519	-8.6	
1-benzoyl-4,5-diphenyl-1H-imidazole	696886	-8.1	
1-benzyl-4-chloro-2-pentyl-5-phenyl-1H-imidazole	774001	-7.9	
1-benzoyl-2,4,5-triphenyl-1H-imidazole	483266	-9.2	
(4Z)-5-hydroxy-1-(1-hydroxy-2-methoxy-1H-imidazol-4-yl)dec-4-en-3-one	982345	-6.4	
(4E)-1-(1H-imidazol-4-yl)hex-4-ene-1,5-diol	407128	-5.8	
Lisinopril	5362119	-7.5	

Table 3.6: Binding affinities of imidazole derivativess with 4ZUD

Compounds	CID	ΔG Energy (Kcal/mol)
1-benzoyl-2-hexyl-4-methoxy-5-methyl-1H-imidazole	560912	-7.6
2-(2-methoxyphenyl)-4,5-diphenyl-1H-imidazole	74782	-9.2
1-benzoyl-2-hexyl-4,5-diphenyl-1H-imidazole	110237	-9
2,4,5-triphenyl-1H-imidazole	10232	-9
2-amino-1-benzoyl-1H-1,3-benzodiazole-5-carboxamide	642519	-8.8
1-benzoyl-4,5-diphenyl-1H-imidazole	696886	-9.7
1-benzyl-4-chloro-2-pentyl-5-phenyl-1H-imidazole	774001	-8.3
1-benzoyl-2,4,5-triphenyl-1H-imidazole	483266	-9.6
(4Z)-5-hydroxy-1-(1-hydroxy-2-methoxy-1H-imidazol-4-yl)dec-4-en-3-one	982345	-6.4
(4E)-1-(1H-imidazol-4-yl)hex-4-ene-1,5-diol	407128	-5.6
Olmesartan	158781	-8.9

Table 3.7: Binding affinities of imidazole derivatives with 5XPR

Compounds	CID	ΔG Energy (Kcal/mol)

1-benzoyl-2-hexyl-4-methoxy-5-methyl-1H-imidazole	560912	-6
2-(2-methoxyphenyl)-4,5-diphenyl-1H-imidazole	74782	-8.1
1-benzoyl-2-hexyl-4,5-diphenyl-1H-imidazole	110237	-7.5
2,4,5-triphenyl-1H-imidazole	10232	-7.9
2-amino-1-benzoyl-1H-1,3-benzodiazole-5-carboxamide	642519	-7.5
1-benzoyl-4,5-diphenyl-1H-imidazole	696886	-7.9
1-benzyl-4-chloro-2-pentyl-5-phenyl-1H-imidazole	774001	-5.5
1-benzoyl-2,4,5-triphenyl-1H-imidazole	483266	-8.3
(4Z)-5-hydroxy-1-(1-hydroxy-2-methoxy-1H-imidazol-4-yl)dec-4-en-3-one	982345	-5.7
(4E)-1-(1H-imidazol-4-yl)hex-4-ene-1,5-diol	407128	-5.2
Bosentan	104865	-8.7

Table 3.8: Binding affinities of imidazole derivatives with 6L88

Compounds	CID	ΔG Energy (Kcal/mol)
1-benzoyl-2-hexyl-4-methoxy-5-methyl-1H-imidazole	560912	-6.5
2-(2-methoxyphenyl)-4,5-diphenyl-1H-imidazole	74782	-8.1
1-benzoyl-2-hexyl-4,5-diphenyl-1H-imidazole	110237	-6.9
2,4,5-triphenyl-1H-imidazole	10232	-8.6
2-amino-1-benzoyl-1H-1,3-benzodiazole-5-carboxamide	642519	-7.9
1-benzoyl-4,5-diphenyl-1H-imidazole	696886	-8.4
1-benzyl-4-chloro-2-pentyl-5-phenyl-1H-imidazole	774001	-6.7
1-benzoyl-2,4,5-triphenyl-1H-imidazole	483266	-7.4
(4Z)-5-hydroxy-1-(1-hydroxy-2-methoxy-1H-imidazol-4-yl)dec-4-en-3-one	982345	-6.8
(4E)-1-(1H-imidazol-4-yl)hex-4-ene-1,5-diol	407128	-5.8
Esaxerenone	25052023	-8.8

The identified imidazole compounds are shown in figures 3.1, 3.2, 3.3, 3.4, .3.5, and 3.6 below

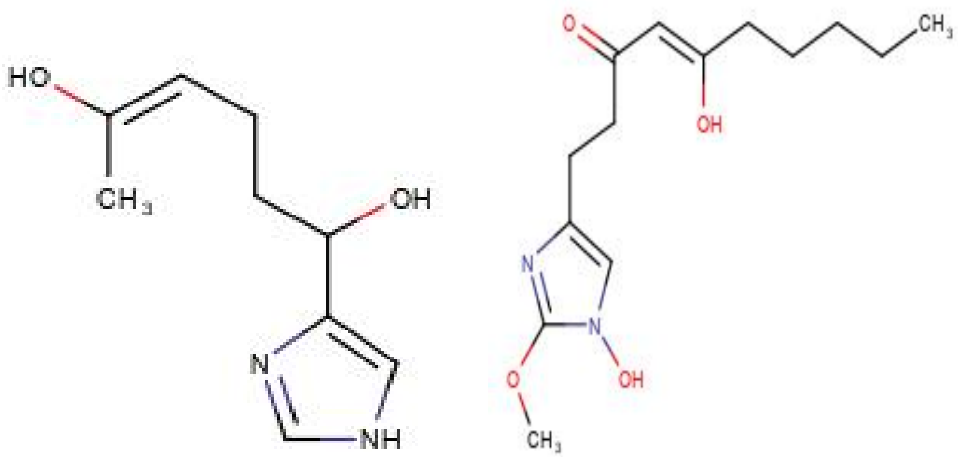

A B

Figure 3.1 Structure of (4Z)-5-hydroxy-1-(1-hydroxy-2-methoxy-1H-imidazol-4-yl)dec-4-en-3-

one(A) and (4E)-1-(1H-imidazol-4-yl)hex-4-ene-1,5-

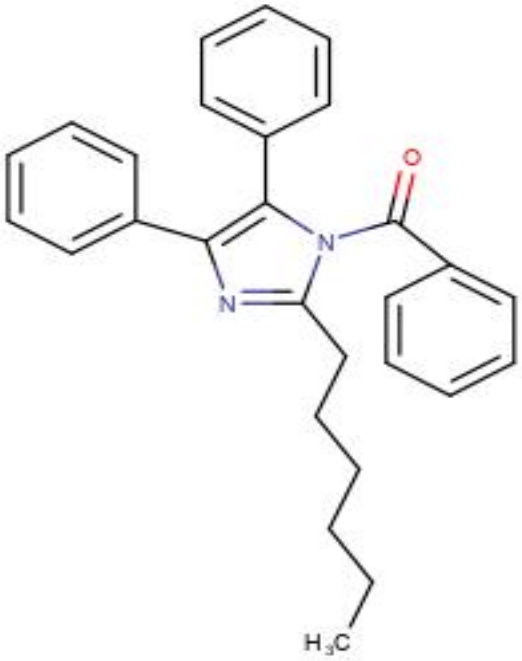

diol(B) A

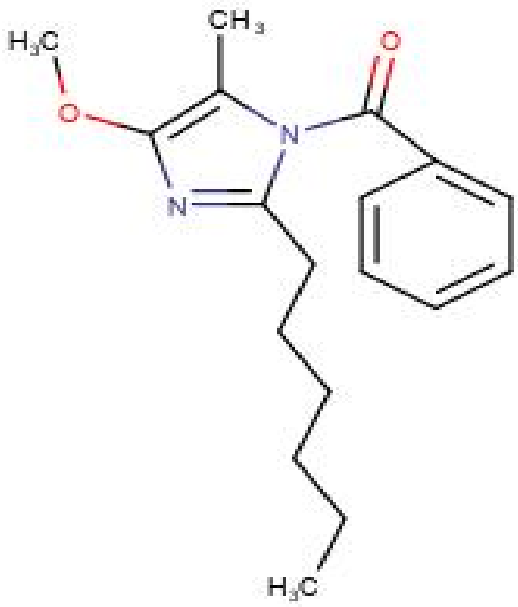

B

Figure 3.2: Structure of 1-benzoyl-2-hexyl-4,5-diphenyl-1H-imidazole (A) and 1-benzoyl-2-hexyl-4-methoxy-5-methyl-1H-imidazole (B)

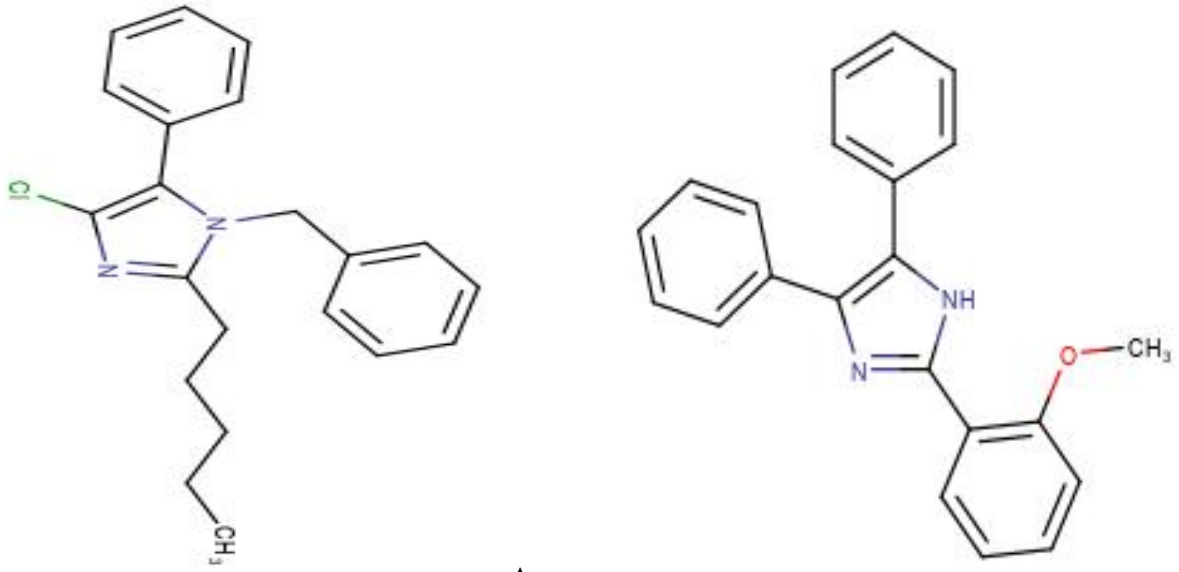

A B

Figure 3.3: Structure of 1-benzyl-4-chloro-2-pentyl-5-phenyl-1H-imidazole(A) and 2-(2-methoxyphenyl)-4,5-diphenyl-1H-imidazole(B)

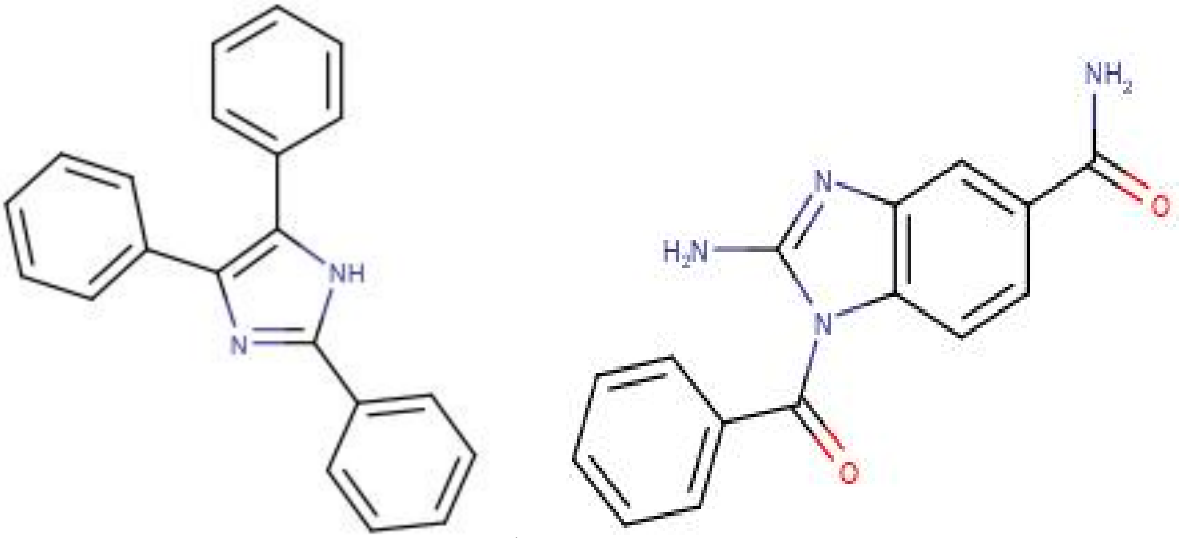

A B

Figure 3.4: Structure of 2,4,5-triphenyl-1H-imidazole(A) and 2-amino-1-benzoyl-1H-1,3-benzodiazole-5-carboxamide(B)

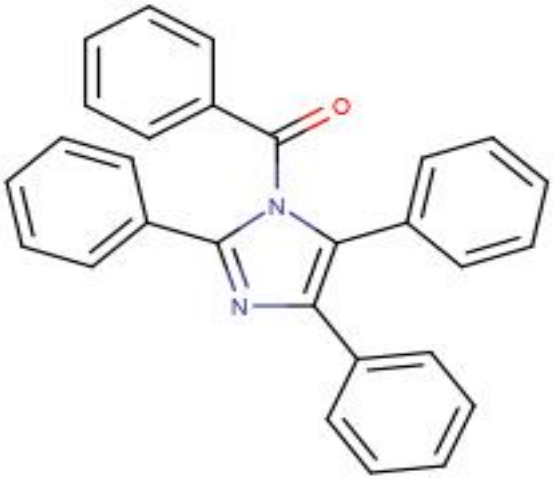

Figure 3.5: Structure of 1-benzoyl-2,4,5-triphenyl-1H-imidazole

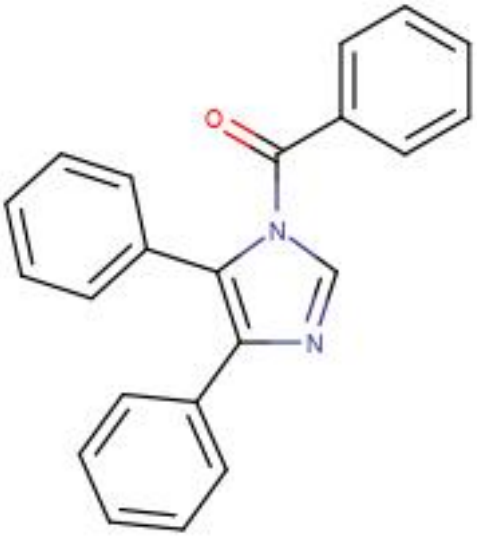

Figure 3.6: Structure of 1-benzoyl-4,5-diphenyl-1H-imidazole

3.2: Binding interactions between the proteins and the ligands

The receptor–ligand interaction analysis revealed distinct binding patterns for the imidazole derivatives across the four target proteins. The binding interactions of the top three ligands with the binding site amino acid residues of each protein target were analyzed in 3D and 2D views can be seen in Figure 3.7, 3.8, 3.9, 3.10, 3.11, 3.12, and 3.13

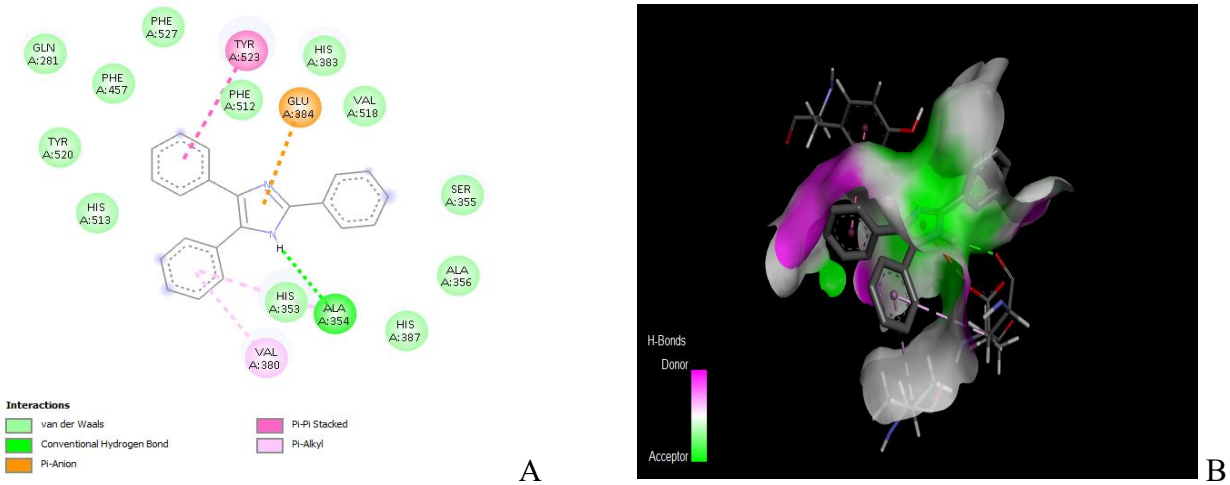

A B

Figure 3.7: Showing 2D (A) and 3D H-bond (B) interactions between protein 1O86 and ligands 2,4,5-triphenyl-1H-imidazole with binding affinity of -9.4

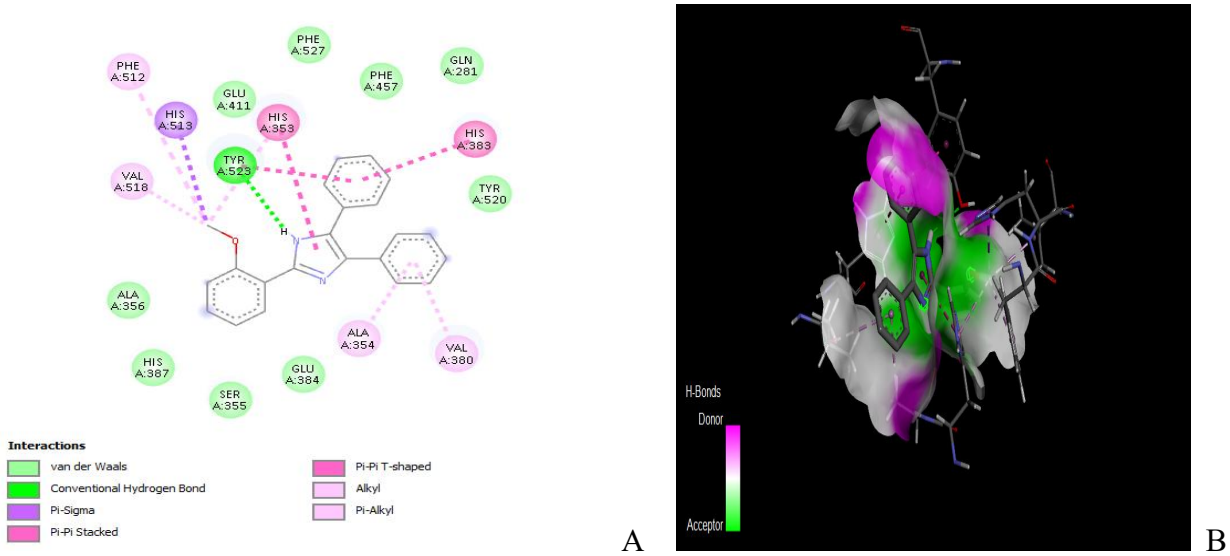

A B

Figure 3.8: Showing 2D (A) and 3D H-bond (B) interactions between protein 1O86 and ligands 2-(2-methoxyphenyl)-4,5-diphenyl-1H-imidazole with binding affinity of -9.7

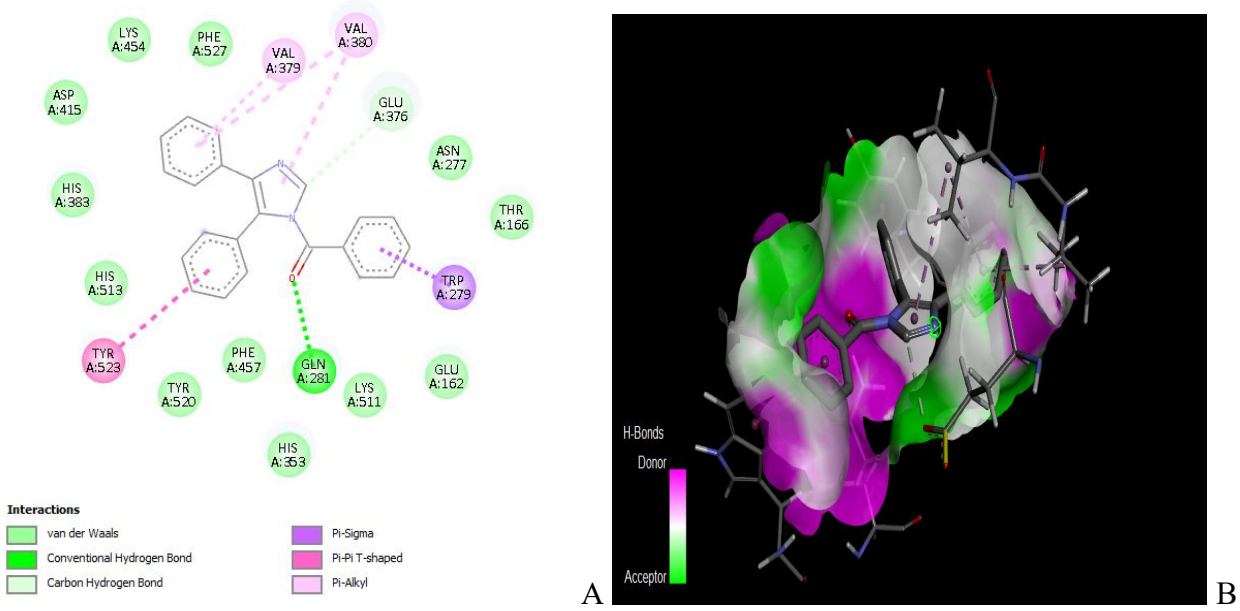

A B

Figure 3.9: Showing 2D (A) and 3D H-bond (B) interactions between protein 1O86 and ligands 1-benzoyl-4,5-diphenyl-1H-imidazole with binding affinity of -9.2..

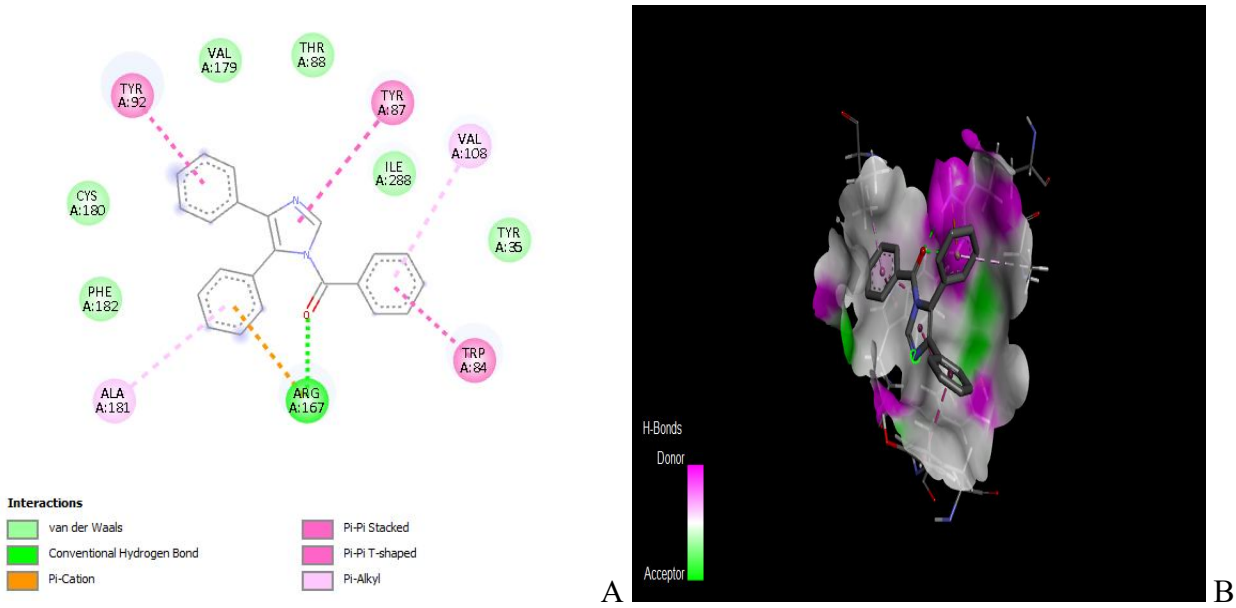

Figure 3.10: Showing 2D (A) and 3D H-bond (B) interactions between protein 4ZUD and ligands 1-benzoyl-4,5-diphenyl-1H-imidazole with binding affinity of -9.7.

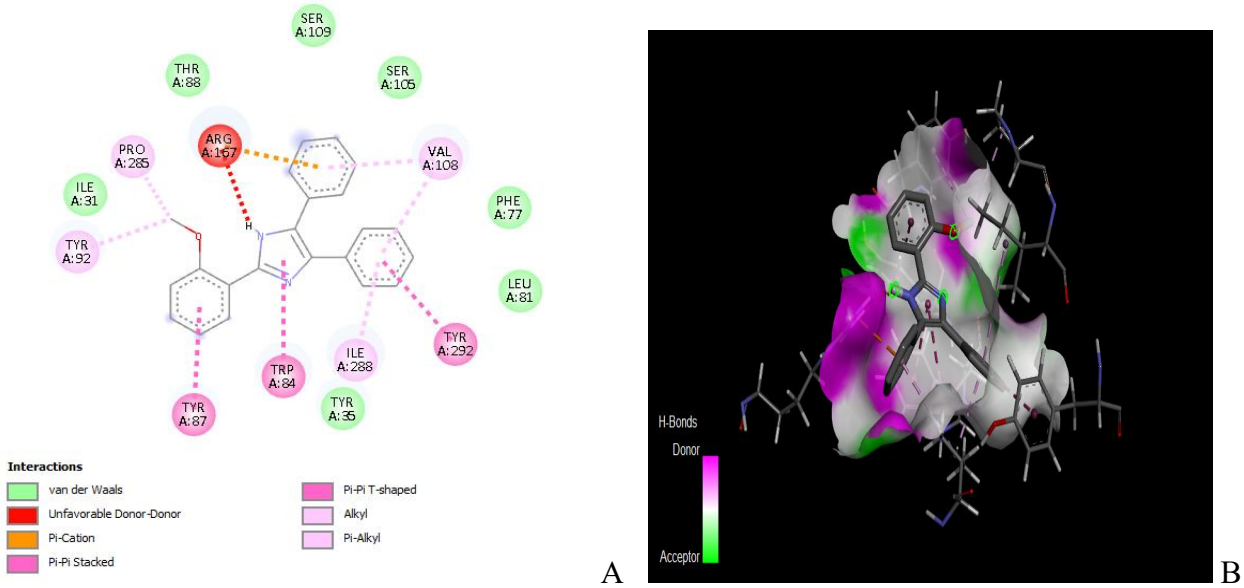

Figure 3.11: Showing 2D (A) and 3D H-bond (B) interactions between protein 4ZUD and ligands 2-(2-methoxyphenyl)-4,5-diphenyl-1H-imidazole with binding affinity of -9.2

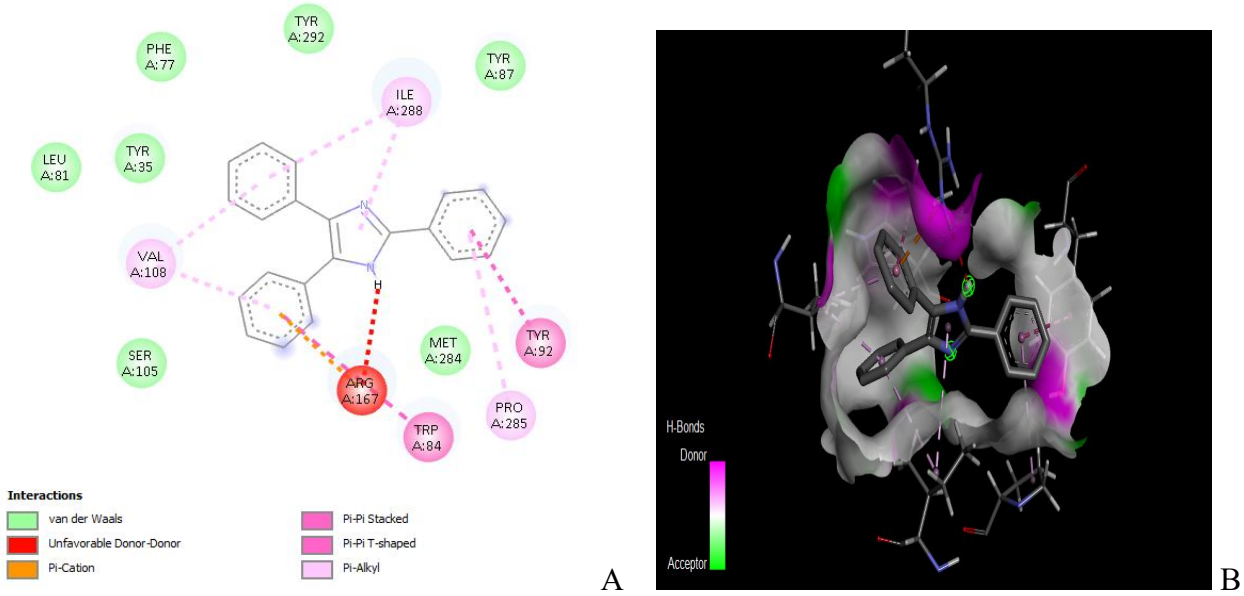

Figure 3.12: Showing 2D (A) and 3D H-bond (B) interactions between protein 4ZUD and ligands 2,4,5-triphenyl-1H-imidazole with binding affinity of -9

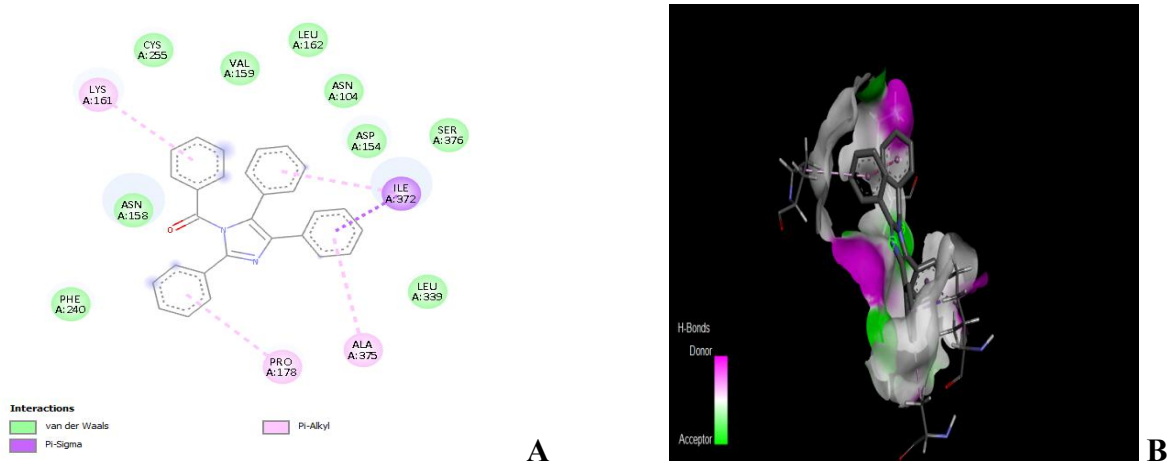

Figure 3.13: Showing 2D (A) and 3D H-bond (B) interactions between protein 5XPR and ligands 1-benzoyl-2,4,5-triphenyl-1H-imidazole with binding affinity of -8.3.

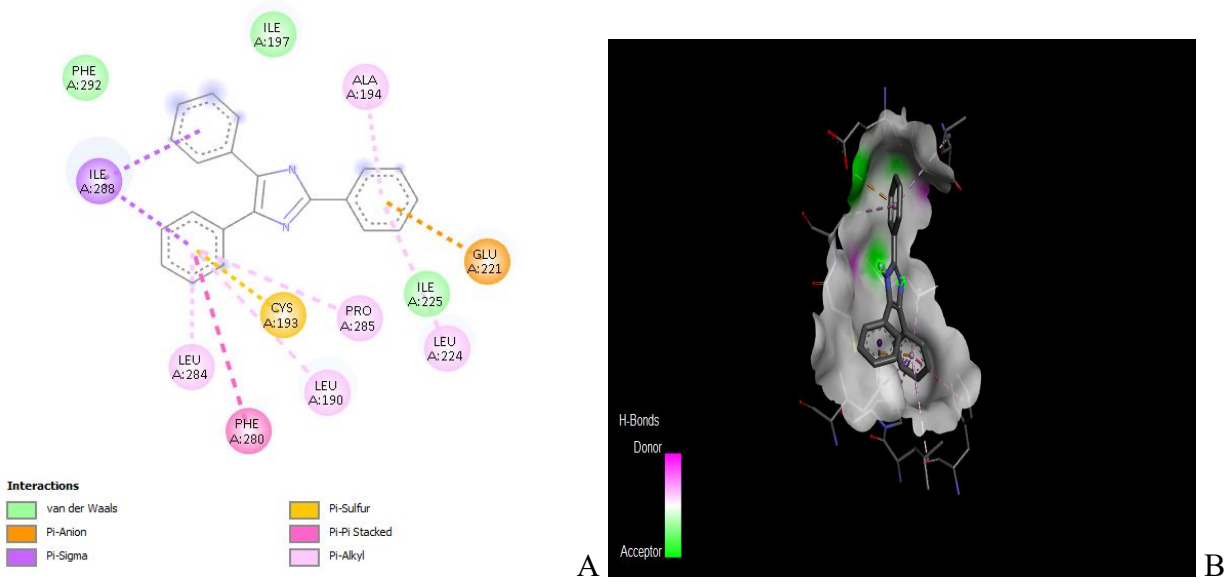

Figure 3.14: Showing 2D (A) and 3D H-bond (B) interactions between protein 5XPR and ligands 2,4,5-triphenyl-1H-imidazole with binding affinity of -7.6

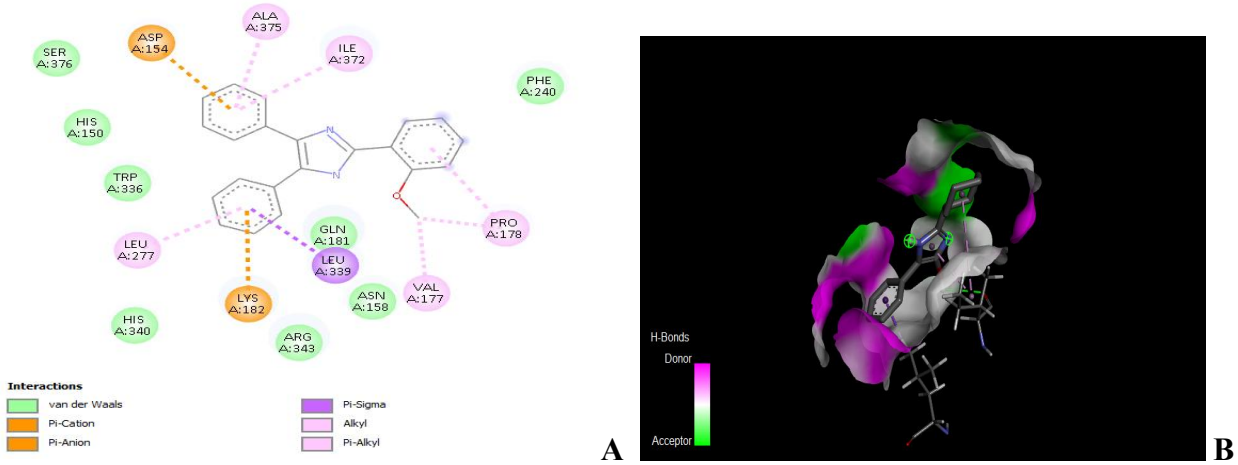

Figure 3.15: Showing 2D (A) and 3D H-bond (B) interactions between protein 5XPR and ligands 2-(2-methoxyphenyl)-4,5-diphenyl-1H-imidazole with binding affinity of -8.1.

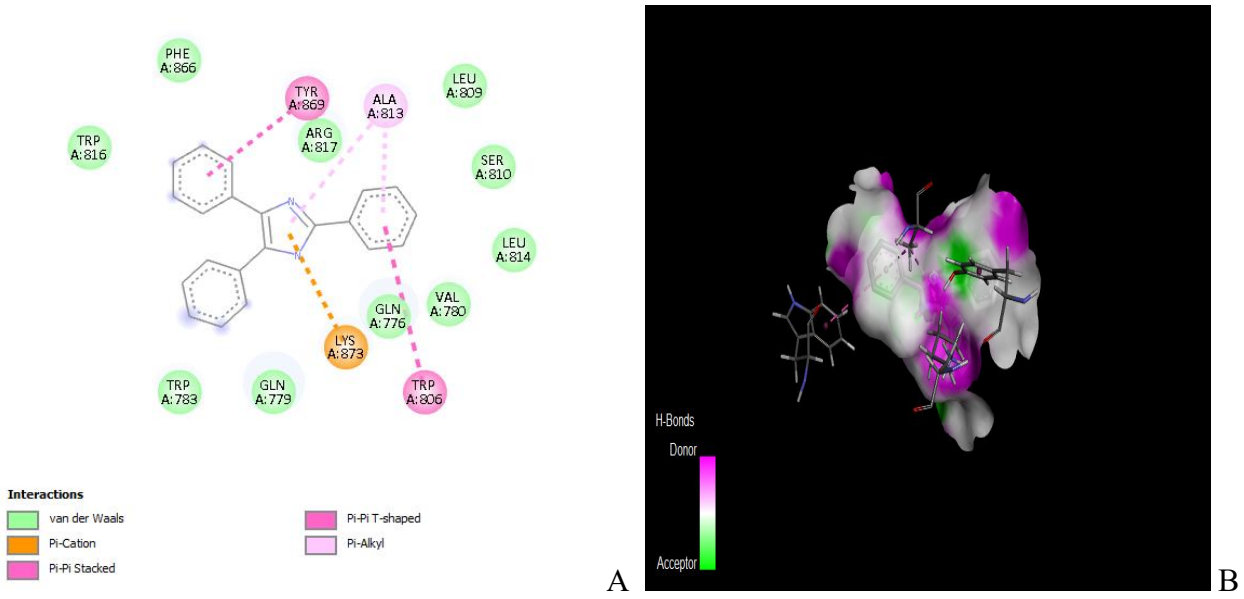

Figure 3.16: Showing 2D (A) and 3D H-bond (B) interactions between protein 6L88 and ligands 2,4,5-triphenyl-1H-imidazole with binding affinity of -8.6

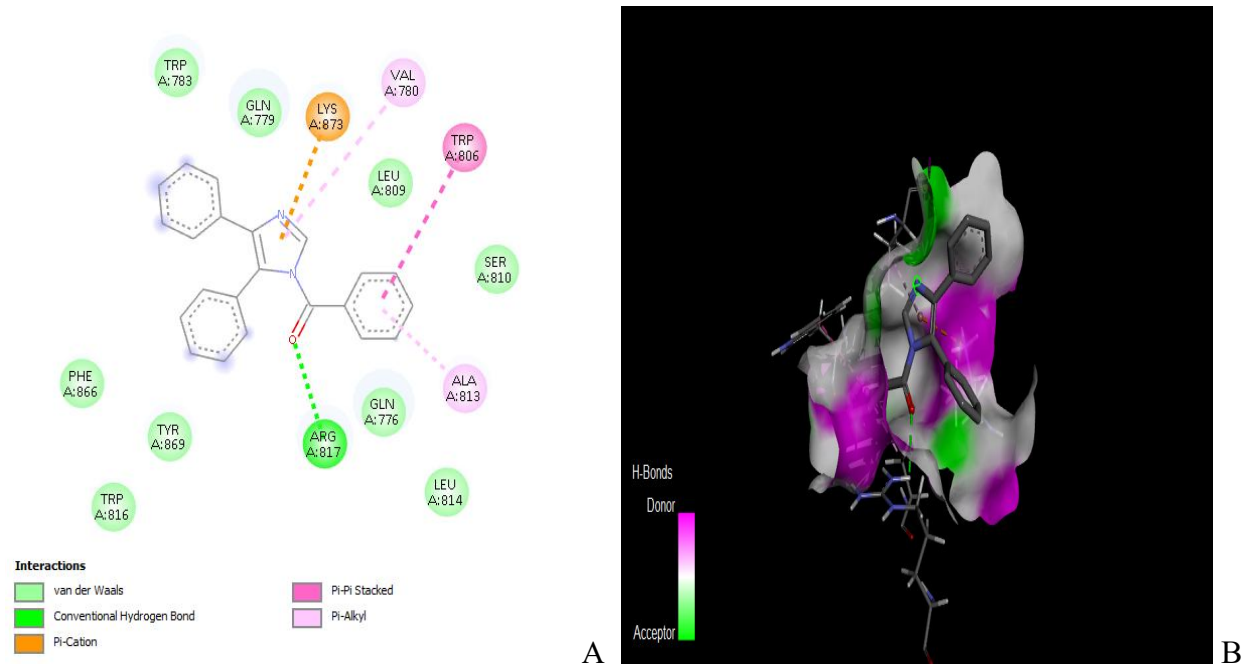

Figure 3.17: Showing 2D (A) and 3D H-bond (B) interactions between protein 6L88 and ligands 1-benzoyl-4,5-diphenyl-1H-imidazole with binding affinity of -8.4.

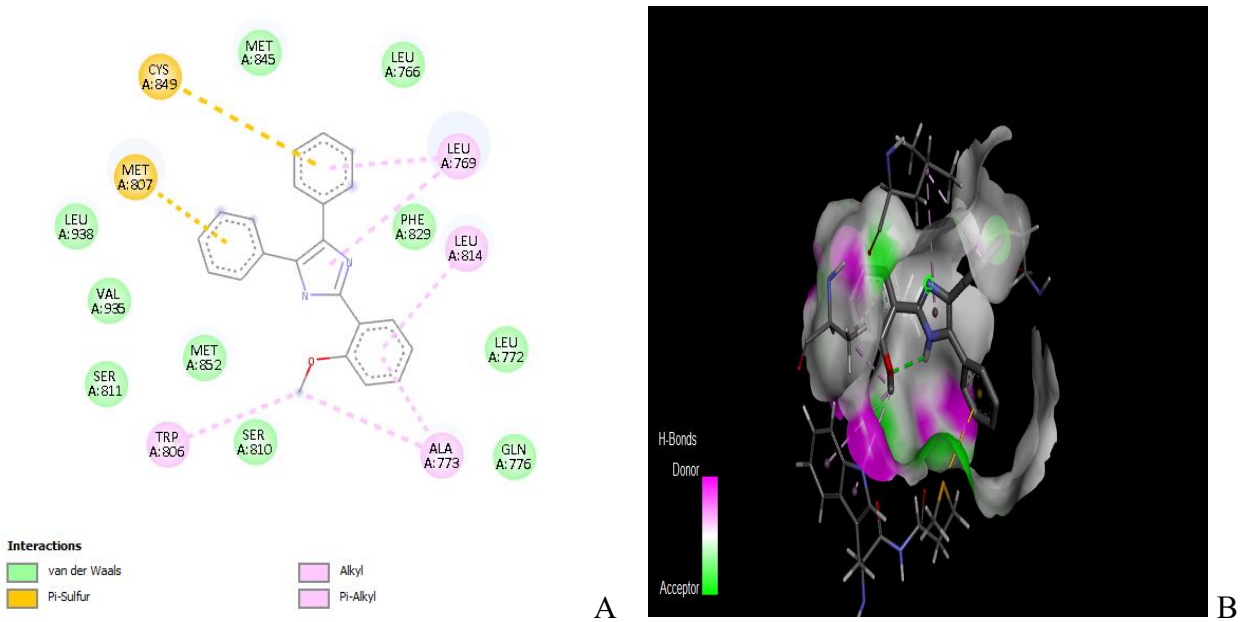

Figure 3.18: Showing 2D (A) and 3D H-bond (B) interactions between protein 6L88 and ligands 2-(2-methoxyphenyl)-4,5-diphenyl-1H-imidazole with binding affinity of -8.1.

3.2 ADME ProfilingTable 3.9: Physicochemical Properties of the Selected Imidazole Compounds.

S/N	Ligands	Formula	Molecular Weight (g/mol)	Num. Heavy Atoms	Fraction CSP3	Num. Rotatable Bonds	Num. H Bond Acceptors	Num. H Bond Donors	Molar Refractivity	TPSA (A^2)
1	407128	C9H14N2O2	182.22	13	0.44	4	3	3	49.85	69.14
2	982345	C14H22N2O4	282.34	20	0.57	9	5	2	75.79	84.58
3	110237	C27H30N2O	398.54	30	0.26	10	2	0	126.87	34.89
4	560912	C18H24N2O2	300.4	22	0.44	8	3	0	88.86	44.12
5	774001	C21H23ClN2	338.87	24	0.29	7	1	0	102.62	17.82
6	74782	C22H18N2O	326.39	25	0.05	4	2	1	101.39	37.91
7	10232	C21H16N2	296.37	23	0	3	1	1	94.9	28.68
8	642519	C15H12N4O2	280.28	21	0	3	3	2	78.4	104
9	696886	C22H16N2O	324.38	25	0	4	2	0	99.27	34.89
10	483266	C28H20N2O	400.47	31	0	5	2	0	124.71	34.89

Table 3.10: Pharmacokinetic Parameters of the Selected Imidazole Compounds

S/N	Ligands	GI Absorption	BBB Permeant	P-gp Substrate	CPY1A2 Inhibitor	CP2C19 Inhibitor	CP2D6 Inhibitor	CP3A4 Inhibitor	Log Kp (Skin permeation (cm/s)
1	407128	High	Yes	No	No	No	No	No	-7.14
2	982345	High	No	No	No	No	No	No	-5.87
3	110237	Low	No	Yes	No	Yes	Yes	No	-2.97
4	560912	High	Yes	No	Yes	Yes	Yes	Yes	-4.53
5	774001	High	No	Yes	Yes	Yes	Yes	Yes	-3.75
6	74782	High	Yes	Yes	Yes	Yes	No	Yes	-4.73
7	10232	High	Yes	Yes	Yes	Yes	No	Yes	-4.52
8	642519	High	No	No	No	No	No	No	-6.55
9	696886	High	Yes	No	Yes	Yes	Yes	No	-4.81
10	483266	High	No	Yes	Yes	Yes	No	No	-4.1

Table 3.11: Lipophilicity Characteristics and Druglikeness of selected imidazole compounds

S/N	Ligands	Lipophilicity (Log Po/w (!LOGP))	Lipophilicity (Log Po/w (XLOGP3))	Lipophilicity (Log Po/w (MLOGP))	Lipophilicity (Log Po/w (SILICOS-IT))	Druglikeness (Lipinski)
1	407128	1.05	0.38	-0.5	1.28	Yes; 0 violation
2	982345	2.86	3.03	0.93	1.76	Yes; 0 violation
3	110237	4.51	8.11	5.14	7.11	Yes; 0 violation
4	560912	3.7	5.07	2.99	4.24	Yes; 0 violation
5	774001	3.84	6.5	4.39	6.03	Yes; 1 violation
6	74782	2.98	5.02	3.56	5.64	Yes; 0violation
7	10232	2.93	5.05	3.95	5.62	Yes; 0 violation
8	642519	1.49	2.06	1.56	0.81	Yes; 0 violation
9	696886	2.95	4.88	4.03	4.47	Yes; 0 violation
10	483266	3.65	6.54	5.33	6	Yes; 1 violation

3.3 Toxicity Prediction

Table 3.12: Toxicity profile of the selected imidazole compounds

S/N	Ligands CID	Hepatotoxicity	Neurotoxicity	Nephro toxicity	Respiratory Toxicity	Cardio toxicity	Carcino genicity	Mutagenicity	Cytotoxicity	LD 50(mg/kg)
1	407128	Inactive	Inactive	Inactive	Active	Inactive	Inactive	Inactive	Inactive	300
2	982345	Inactive	Inactive	Active	Active	Inactive	Inactive	Inactive	Inactive	911
3	110237	Inactive	Active	Inactive	Active	Inactive	Inactive	Inactive	Inactive	1150
4	560912	Inactive	Active	Inactive	Active	Inactive	Inactive	Inactive	Inactive	298
5	774001	Inactive	Active	Inactive	Active	Inactive	Inactive	Inactive	Inactive	1152
6	74782	Active	Active	Inactive	Active	Inactive	Active	Active	Inactive	2000
7	10232	Active	Active	Inactive	Active	Inactive	Inactive	Inactive	Inactive	300
8	642519	Active	Active	Inactive	Active	Inactive	Active	Active	Inactive	650
9	696886	Inactive	Active	Inactive	Active	Inactive	Inactive	Inactive	Inactive	1150
10	483266	Inactive	Active	Inactive	Active	Inactive	Inactive	Inactive	Inactive	1152

3.3 Result of Synthesis

The reaction between benzil, ammonium acetate and benzaldehyde led to the synthesis of 2,4,5-triphenyl-1H-imidazole as shown in figure 3.1 below

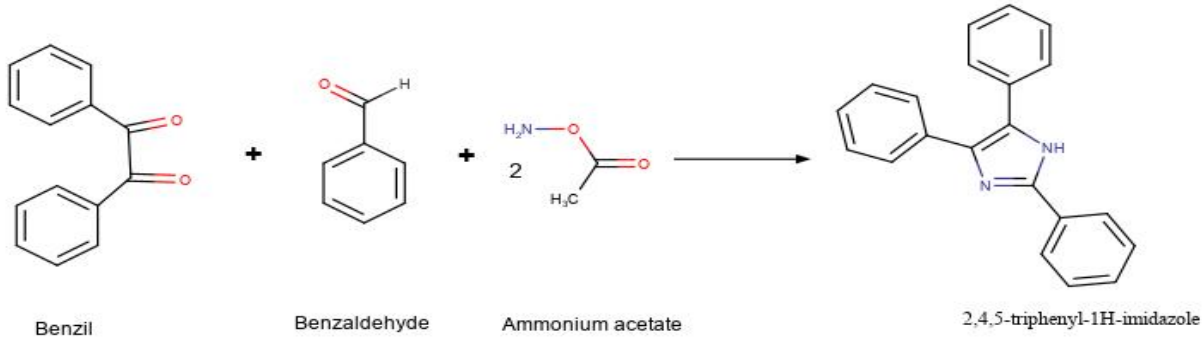

Figure 3.19: Scheme of reaction for synthesis of 2,4,5-triphenyl-1H-imidazole

Molecular weight: 296.37g/mol

Yield: 3.01g

3.3.1 Organoleptic Properties

Table 3.13: Organoleptic Properties of synthesized of 2,4,5-triphenyl-1H-imidazole

Sample code	Colour	Smell	Texture
TPI	White	Characteristic	Soft & Smooth

3.3.2 Percentage Yield and Melting Point

Table 3.14: Percentage Yield and Melting Point of synthesized of 2,4,5-triphenyl-1H-imidazole

Sample code	Percentage Yield	Melting Point
TPI	81.28 %	269-272^{0}C

Spectroscopic Analysis: The sample was submitted for spectroscopic analysis; however, the results were not available at the time this paper was prepared.

CHAPTER FOUR

DISCUSSION

Molecular docking is a key computational technique used to predict the preferred orientation and binding affinity of a ligand when interacting with a protein receptor at the molecular level. By estimating the strength and stability of ligand–receptor complexes, docking provides insight into how small molecules may modulate protein function, and is therefore essential in structure-based drug discovery (Morris & Lim-Wilby, 2024). This approach is particularly valuable in the search for new therapeutic agents where experimental screening may be costly, time-consuming, or limited by accessibility to biological assay systems. The limitations of current hypertension therapies highlight the need for new, safer and affordable antihypertensive agents. Imidazole derivatives are promising because their ring system supports strong molecular interactions with biological targets. Their presence in several clinically used drugs underscores their potential as leads for antihypertensive drug development

4.1: Protein active site identification

Active site identification is an essential step in structure-based drug design because ligand binding occurs at specific amino acid residues that influence protein function For the proteins analyzed (PDB IDs: 1O86, 4ZUD, 5XPR, and 6L88) and their respective native ligands (lisinopril, olmesartan, bosentan, and esaxerenone), the identified active site pockets were composed of key amino acid residues including phenylalanine, leucine, glutamic acid, alanine, methionine, isoleucine, tyrosine, arginine, tryptophan, cysteine, glutamine, asparagine, valine, and proline. Aromatic residues like phenylalanine, tyrosine, and tryptophan contribute to π–π stacking and hydrophobic interactions, while charged residues such as arginine and glutamic acid enable hydrogen bonding and electrostatic stabilization (Du et al., 2016)

Lisinopril is an ACE inhibitor that blocks the conversion of angiotensin I to angiotensin II, a potent vasoconstrictor. By inhibiting ACE, lisinopril reduces vascular resistance and lowers blood pressure. Olmesartan is an angiotensin II type 1 receptor (AT1R) blocker, preventing angiotensin II from binding to its receptor. This interference reduces vasoconstriction and aldosterone release, promoting vasodilation (Carey & Whelton 2018). Bosentan is a dual endothelin receptor antagonist, primarily targeting endothelin receptor type A. By blocking endothelin-mediated vasoconstriction, bosentan improves blood flow, especially in pulmonary hypertension. Esaxerenone acts as a non-steroidal mineralocorticoid receptor antagonist. It blocks aldosterone-induced sodium retention and vascular remodeling, leading to lowered blood pressure (Correale et al., 2025; Hafez et al., 2025). Together, these drugs represent four distinct mechanisms of antihypertensive action, providing meaningful comparators for evaluating the therapeutic potential of the imidazole derivatives.

4.2: Binding affinity

As presented in Table 3.9, 3.10, 3.11 and 3.12 a total of eleven (11) compounds, including the standard reference and the native ligand interacted with each target protein with binding affinities ranges; 1O86 (–5.8 to –9.7 kcal/mol), 4ZUD (–5.6 to –9.7 kcal/mol), 5XPR(–5.2 to –8.7 kcal/mol) and 6L88 (–5.8 to –8.9 kcal/mol). The docking analysis compared the binding affinities of the synthesized imidazole derivatives with standard antihypertensive drugs (lisinopril, olmesartan, bosentan, and esaxerenone) across the target proteins 1O86, 4ZUD, 5XPR, and 6L88. Against protein 1O86, the compounds 2-(2-methoxyphenyl)-4,5-diphenyl-1H-

that imidazole, 2,4,5-triphenyl-1H-imidazole, and 1-benzoyl-4,5-diphenyl-1H-imidazole exhibited the most favorable binding affinities of -9.7, -9.4, and -9.2 kcal/mol, respectively. Whereas 1-benzoyl-2-hexyl-4-methoxy-5-methyl-1H-imidazole, (4Z)-5-hydroxy-1-(1-hydroxy-

2-methoxy-1H-imidazol-4-yl)dec-4-en-3-one and (4E)-1-(1H-imidazol-4-yl)hex-4-ene-1,5-diol had binding affinities lower than lisinopril (-7.5 kcal/mol), others demonstrated binding affinities equal to or more negative than that value.

Similarly, strong binding was observed on 4ZUD, where 1-benzoyl-4,5-diphenyl-1H-imidazole, 1-benzoyl-2,4,5-triphenyl-1H-imidazole, 2-(2-methoxyphenyl)-4,5-diphenyl-1H-imidazole, and 2,4,5-triphenyl-1H-imidazole, 1-benzoyl-2-hexyl-4,5-diphenyl-1H-imidazole having a binding affinity of -9.7, -9.6,-9.2, and -9 kcal/mol while others had lower binding score than (-8.9 kcal/mol).

For 5XPR, notable binding was observed with 1-benzoyl-2,4,5-triphenyl-1H-imidazole (-8.3 kcal/mol), 2-(2-methoxyphenyl)-4,5-diphenyl-1H-imidazole (-8.1 kcal/mol), 1-benzoyl-4,5-diphenyl-1H-imidazole and 2,4,5-triphenyl-1H-imidazole (-7.9 kcal/mol), though all the derivative demonstrated binding affinities less than the reference drug bosentan (-8.7 kcal/mol).

With target protein 6L88, the compounds demonstrated good affinity (-8.1 to -8.6 kcal/mol), their binding scores were slightly less negative than that of the standard drug esaxerenone (-8.8 kcal/mol), suggesting that while the derivatives interact favorably, their inhibitory potential on this target may be comparatively lower.

In molecular docking, more negative binding energy values indicate stronger and more favorable ligand–protein interactions. This suggests that ligands with lower binding energy are more likely to form stable complexes with the target protein. Therefore, the imidazole derivatives exhibited more negative binding energies than the reference ligands may potentially demonstrate stronger binding affinity and improved interaction stability within the active site. This highlights their potential to act as effective inhibitors. However, binding affinity alone is not sufficient to

establish a compound as a viable drug candidate. Factors such as selectivity, pharmacokinetics, ADMET profile, and toxicity must also be favorable to ensure safety, efficacy, and therapeutic relevance.

In the post docking analysis, 2,4,5-triphenyl-1H-imidazole showed that its interactions across the studied protein targets were largely driven by hydrophobic contacts. In 1O86, the compound formed several van der Waals interactions supported by a single conventional hydrogen bond with amino acid, suggesting a stable but mostly nonpolar binding mode. For 4ZUD, the ligand also interacted mainly through van der Waals forces, though an unfavorable interaction with Arg167 may slightly weaken its affinity. In proteins 5XPR and 6L88, similar nonpolar interactions dominated, with no notable hydrogen bonds observed indicating that ligand binds effectively through hydrophobic stabilization.

1-benzoyl-4,5-diphenyl-1H-imidazole interacts favorably within the binding pockets of the target proteins 1O86, 4ZUD, 5XPR, and 6L88. In the 6L88 protein, the compound formed an additional conventional hydrogen bond with ARG817, which enhances binding specificity and may improve inhibitory potential. 2-(2-methoxyphenyl)-4,5-diphenyl-1H-imidazole demonstrated notable interactions across the binding pockets of the target proteins 1O86, 4ZUD, 5XPR, and 6L88. In the 1O86 binding pocket, an additional conventional hydrogen bond was formed with GLN281, which likely contributes to enhanced binding stability and specificity. However, in the 4ZUD complex, an unfavorable donor–donor interaction was observed with ARG167, which may reduce binding affinity or contribute to steric hindrance at that site.

Overall, the results suggest that specific imidazole derivatives, particularly those bearing benzoyl and triphenyl substitutions, exhibit promising binding characteristics on multiple hypertension-

related protein targets and may serve as potential lead candidates for further biological evaluation.

4.3: ADMET Properties of the Imidazole Compounds.

ADME (Absorption, Distribution, Metabolism, and Excretion) evaluation is essential in predicting the drug-likeness of candidate molecules before synthesis, thereby reducing the risk of pharmacokinetic failure during drug development. Several theoretical rules exist for assessing drug-likeness; however, this study adopted Lipinski's Rule of Five. According to this rule, an orally active compound should not violate more than one of the following criteria: it should have no more than 5 hydrogen bond donors, 10 hydrogen bond acceptors, a molecular weight of 500 Da or less, and an octanol–water partition coefficient (log P) not exceeding 5.

From the result summarized in table 3.5, 3.6 and 3.7,most of the compounds in this study complied with Lipinski's thresholds, indicating favorable physicochemical characteristics for oral drug development. Specifically, compounds such as (4E)-1-(1H-imidazol-4-yl)hex-4-ene-1,5-diol, (4Z)-5-hydroxy-1-(1-hydroxy-2-methoxy-1H-imidazol-4-yl)dec-4-en-3-one, 1-benzoyl-2-hexyl-4-methoxy-5-methyl-1H-imidazole, 2,4,5-triphenyl-1H-imidazole and 2-amino-1-benzoyl-1H-1,3-benzodiazole-5-carboxamide showed no Lipinski violations. These compounds exhibited molecular weights below 500 g/mol, LogP values within the acceptable range (≤ 5), and acceptable numbers of hydrogen bond donors and acceptors, suggesting strong potential for oral bioavailability.

However, derivatives bearing extensive aromatic substitution and bulky hydrophobic groups, including 1-benzoyl-2-hexyl-4,5-diphenyl-1H-imidazole, 1-benzyl-4-chloro-2-pentyl-5-phenyl-1H-imidazole, and 1-benzoyl-2,4,5-triphenyl-1H-imidazole, showed markedly high LogP values

(>5). Although their molecular weights remained within acceptable limits, the elevated lipophilicity resulted in poor predicted aqueous solubility, which may reduce oral absorption and limit systemic exposure. These compounds may require structural modification or specialized formulation strategies to enhance bioavailability.

The majority of the imidazole derivatives demonstrated high GI absorption, indicating that these compounds are likely to be efficiently absorbed when administered orally. This is a favorable property in drug development because it suggests good bioavailability and supports the potential for oral dosing. However, one compound (1-benzoyl-2-hexyl-4,5-diphenyl-1H-imidazole) exhibited low GI absorption, suggesting reduced oral bioavailability. Such a compound may require formulation enhancement, or an alternative administration route to improve systemic uptake

BBB permeability varied among the compounds, indicating differences in their ability to cross into the central nervous system. Several compounds (e.g., Ligands (4E)-1-(1H-imidazol-4-yl)hex-4-ene-1,5-diol, 1-benzoyl-2-hexyl-4-methoxy-5-methyl-1H-imidazole, 2-(2-methoxyphenyl)-4,5-diphenyl-1H-imidazole, 2,4,5-triphenyl-1H-imidazole, 1-benzoyl-4,5-diphenyl-1H-imidazole) were predicted to be BBB permeant, suggesting they may exert central nervous system (CNS) effects or could be explored for CNS-related therapeutic use. Others were not BBB permeant, implying limited brain penetration, which may be advantageous for antihypertensive therapy since most cardiovascular drugs do not require central action and reduced CNS exposure lowers the risk of neurological side effects.

P-gp is an efflux transporter that pumps drugs out of cells, affecting absorption, distribution, and resistance. Several compounds (e.g., 1-benzoyl-2-hexyl-4,5-diphenyl-1H-imidazole, 1-benzyl-4-

chloro-2-pentyl-5-phenyl-1H-imidazole, 2-(2-methoxyphenyl)-4,5-diphenyl-1H-imidazole, 2,4,5-triphenyl-1H-imidazole, 1-benzoyl-2,4,5-triphenyl-1H-imidazole) were predicted to be P-gp substrates.This means they are likely to be actively transported out of intestinal and brain cells, which may reduce intracellular drug concentration and lower oral bioavailability. Other compounds were not P-gp substrates, suggesting they may have more stable systemic retention and potentially improved bioavailability. Compounds that act as P-gp substrates may show reduced therapeutic efficacy unless

4.4: Toxicity Profiles of the Imidazole Compounds

The toxicity profiling of the imidazole-based derivatives revealed varied safety patterns across organ systems. Most compounds showed no nephrotoxicity, cardiotoxicity, mutagenicity, carcinogenicity, or cytotoxicity, indicating a generally favorable baseline safety profile. However, respiratory toxicity and neurotoxicity were consistently active in many derivatives, suggesting possible interactions with neuronal signaling pathways or reactive metabolites affecting pulmonary tissues.

Notably, 2-(2-methoxyphenyl)-4,5-diphenyl-1H-imidazole and 2-amino-1-benzoyl-1H-1,3-benzodiazole-5-carboxamide exhibited hepatotoxicity and carcinogenicity. 2,4,5-triphenyl-1H-imidazole demonstrated hepatotoxic and neurotoxic tendencies but remained non-mutagenic and non-cytotoxic, suggesting manageable risk with structural optimization. Compounds such as 1-benzoyl-4,5-diphenyl-1H-imidazole and 1-benzoyl-2,4,5-triphenyl-1H-imidazole displayed the most favorable safety profiles, being inactive across major toxicity endpoints except respiratory toxicity.

According to the ProTox III toxicity classification system, none of the imidazole derivatives investigated fell into the non-toxic Class VI category. The compounds 2,4,5-triphenyl-1H-imidazole, (4E)-1-(1H-imidazol-4-yl)hex-4-ene-1,5-diol, and 1-benzoyl-2-hexyl-4-methoxy-5-methyl-1H-imidazole were classified under Class III, indicating that they are toxic if swallowed (LD_{50} between 50 and 300 mg/kg). All remaining derivatives were placed in Class IV, which corresponds to compounds considered harmful if swallowed (LD_{50} between 300 and 2000 mg/kg). While these toxicity levels do not preclude their potential therapeutic use, they highlight the need for further structural optimization and safety evaluation to reduce toxicity and improve their suitability as drug candidates.

4.5 Synthesis of 2,4,5-Triphenyl-1H-Imidazole

The synthesis of 2,4,5-triphenyl-1H-imidazole was based on its favorable in silico performance, particularly its strong binding affinity toward the selected protein targets and ADME evaluation which indicated acceptable drug-likeness, including good oral bioavailability and physicochemical stability suitable for further development. ProTox toxicity predictions showed low likelihood of mutagenicity and carcinogenicity, suggesting a safer profile compared to some related derivatives.

2,4,5-Triphenyl-1H-imidazole was synthesized through a modified Debus–Radziszewski imidazole synthesis, involving the condensation of benzil (1,2-diketone), benzaldehyde, and ammonium acetate in glacial acetic acid under reflux. In this reaction, benzil provides the 1,2-dicarbonyl unit, ammonium acetate acts as the ammonia source forming the imine nitrogens, and benzaldehyde contributes the substituent at the C-2 position of the imidazole ring.

The formation of 2,4,5-triphenyl-1H-imidazole in this study proceeds through a condensation–cyclization–aromatization. In the initial stage, ammonium acetate dissociates to release ammonia, which undergoes condensation with benzaldehyde to produce a benzylidene imine intermediate. Concurrently, ammonia interacts with the diketone groups of benzil, generating additional imine-type intermediates that orient the reactants for ring formation. During the cyclization step, the benzylidene imine nucleophilically attacks one of the carbonyl carbons of benzil, leading to the formation of a cyclic imidazoline intermediate. This step establishes the core five-membered ring characteristic of the imidazole structure. The intermediate subsequently undergoes dehydration, a process facilitated by the elevated temperature and acidic conditions, resulting in the elimination of water molecules. Final aromatization occurs through oxidation within the reaction environment, yielding the stable aromatic imidazole ring system.

Glacial acetic acid plays a crucial role in this transformation. It acts as both a protic solvent and a mild acid catalyst, promoting imine formation, stabilizing charged intermediates, and enhancing the cyclization and dehydration steps. Additionally, its high boiling point supports sustained reflux, thereby driving the reaction to completion and improving product yield.

The reaction produced a white, soft, and smooth solid with a characteristic mild odor after recrystallization. The high percentage yield of 81.28% indicates that the reaction pathway proceeded efficiently with minimal side-product formation, suggesting favorable reaction conditions and good reagent compatibility. The narrow melting point range of 269–272°C implies low levels of impurities and supports the stability of the synthesized compound.

4.6 Limitation and Recommendation

This study was limited by its reliance on in silico screening tools, which provide predictive toxicity and activity profiles but may not fully replicate biological responses in vivo. The absence of in vitro and in vivo pharmacological testing prevents confirmation of antihypertensive activity and safety. Only one compound (2,4,5-triphenyl-1H-imidazole) was experimentally synthesized, limiting comparative analysis with other promising derivatives identified during virtual screening. Also advanced structural confirmation techniques such as NMR, FT-IR, and Mass Spectrometry were in not performed in time due to instrument availability constraints.

Future work may focus on optimizing reaction conditions further and explore alternative synthesis pathways, which may further enhance purity and reduce the melting range variation. In vitro biological evaluation should be conducted to validate the compound's predicted antihypertensive potential, followed by in vivo studies to assess pharmacokinetics and safety. Structural modification around the phenyl substituents may also be explored to improve solubility and biological activity.

CHAPTER FIVE

CONCLUSION

This study investigated the binding affinities of selected imidazole derivatives against four hypertension-related protein targets, with lisinopril, bosentan, olmesartan, and esaxerenone serving as reference standards. Molecular docking results identified 2,4,5-triphenyl-1H-imidazole, 1-benzoyl-4,5-diphenyl-1H-imidazole, and 2-(2-methoxyphenyl)-4,5-diphenyl-1H-imidazole as strong candidates, demonstrating favorable interactions and potential antihypertensive activity. The ADME/T analysis indicated that these compounds possess desirable pharmacokinetic and pharmacodynamic properties.

2,4,5-Triphenyl-1H-imidazole demonstrated the most favorable performance across all evaluated parameters, including binding affinity and ADME properties. Based on this, it was selected for laboratory synthesis. The compound was successfully synthesized using the described reaction procedure, yielding a final product with a percentage yield of 81.28%. This high yield indicates that the synthetic route is efficient and reproducible, further supporting the compound's suitability for continued investigation and biological evaluation.

REFERENCES

Abdallah, S., Darweesh, K.M. & Loksha, Y.M., 2024. A review: Imidazole and its biological activities. *Records of Pharmaceutical and Biomedical Sciences*, 8(1), pp.123–129. https://doi.org/10.21608/rpbs.2024.294154.1301

Aburto, N.J., Ziolkovska, A., Hooper, L., Elliott, P., Cappuccio, F.P. & Meerpohl, J.J., 2013. Effect of lower sodium intake on health: Systematic review and meta-analyses. *BMJ*, 346, f1326. DOI: 10.1136/bmj.f1326.

Adeloye, D., Basquill, C., Aderemi, A.V., Thompson, J.Y. & Obi, F.A., 2015. An estimate of the prevalence of hypertension in Nigeria: A systematic review and meta-analysis. *Journal of Hypertension*, 33(2), pp.230–242. DOI: 10.1097/HJH.0000000000000413.

Agarwal, U., Tonk, R.K. & Paliwal, S., 2025. Importance of computer-aided drug design in modern pharmaceutical research. *Current Drug Discovery Technologies*, 22(3), e15701638361318. DOI: 10.2174/0115701638361318241230073123.

ALLHAT Officers and Coordinators for the ALLHAT Collaborative Research Group, 2002. Major outcomes in high-risk hypertensive patients randomized to angiotensin-converting enzyme inhibitor or calcium channel blocker vs diuretic. *JAMA*, 288(23), pp.2981–2997. DOI: 10.1001/jama.288.23.2981.

Ambrosino, P., Bachetti, T., D'Anna, S.E., Galloway, B., Bianco, A., D'Agnano, V., Papa, A., Motta, A., Perrotta, F. & Maniscalco, M., 2022. Mechanisms and clinical implications of endothelial dysfunction in arterial hypertension. *Journal of Cardiovascular Development and Disease*, 9(5), p.136. DOI: 10.3390/jcdd9050136.

Appel, L.J., Frohlich, E.D., Hall, J.E., Pearson, T.A., Sacco, R.L., Seals, D.R. & Whelton, P.K., 2011. The importance of population-wide sodium reduction as a means to prevent cardiovascular disease and stroke: A call to action from the American Heart Association. *Circulation*, 123(10), pp.1138–1143. DOI: 10.1161/CIR.0b013e31820d0793.

Appel, L.J., Moore, T.J., Obarzanek, E. et al., 2011. A clinical trial of the effects of dietary patterns on blood pressure. *New England Journal of Medicine*, 336(16), pp.1117–1124. DOI: 10.1056/NEJM199704173361601.

Awasthi, A., Rahman, M.A. & Bhagavan Raju, M., 2023. Synthesis, In Silico Studies, and In Vitro Anti-Inflammatory Activity of Novel Imidazole Derivatives Targeting p38 MAP Kinase. *ACS Omega*, 8(20), pp.17788–17799. DOI: 10.1021/acsomega.3c00605.

Banerjee, P., Eckert, A.O., Schrey, A.K. & Preissner, R., 2018. ProTox-II: a webserver for the prediction of toxicity of chemicals. *Nucleic Acids Research*, 46(W1), pp.W257–W263. DOI: 10.1093/nar/gky318.

Bangalore, S., Messerli, F.H., Kostis, J.B. & Pepine, C.J., 2007. Cardiovascular protection using β-blockers: A critical review of the evidence. *Journal of the American College of Cardiology*, 50(7), pp.563–572. DOI: 10.1016/j.jacc.2007.04.060.

Brook, R.D., et al., 2013. Beyond medications and diet: Alternative approaches to lowering blood pressure. *Hypertension*, 61(6), pp.1360–1383. DOI: 10.1161/HYP.0b013e318293645f.

Burley, S.K., Bhikadiya, C., Bi, C., Bittrich, S., Chao, H., Chen, L. et al., 2022. RCSB Protein Data Bank: Tools for visualizing and understanding biological macromolecules in 3D. *Protein Science*, 31(12), e4482. doi:10.1002/pro.4482.

Carey, R.M. & Whelton, P.K.; 2017 ACC/AHA Hypertension Guideline Writing Committee, 2018. Prevention, detection, evaluation, and management of high blood pressure in adults: Synopsis of the 2017 American College of Cardiology/American Heart Association Hypertension Guideline. *Annals of Internal Medicine*, 168(5), pp.351–358. DOI: 10.7326/M17-3203.

Carretero, O.A. & Oparil, S., 2000. Essential hypertension: Part I—Definition and etiology. *Circulation*, 101(3), pp.329–335. DOI: 10.1161/01.CIR.101.3.329.

Cohn, J. N., McInnes, G. T., & Shepherd, A. M. (2011). Direct-acting vasodilators. *The Journal of Clinical Hypertension*, 13(9), 690–692. https://doi.org/10.1111/j.1751-7176.2011.00507.x

Correale, M., Mercurio, V., Bevere, E.M.L., Pezzuto, B., Tricarico, L., Attanasio, U., 2025. Pathophysiology of pulmonary arterial hypertension: focus on vascular endothelium as a potential therapeutic target. *International Journal of Molecular Sciences*, 26(19), p.9631. DOI: 10.3390/ijms2619963.

Daina, A., Michielin, O. & Zoete, V., 2017. SwissADME: A free web tool to evaluate pharmacokinetics, drug-likeness and medicinal chemistry friendliness of small molecules. *Scientific Reports*, 7, p.42717. doi:10.1038/srep42717.

Dallakyan, S. & Olson, A.J., 2015. Small-molecule library screening by docking with AutoDock. In: Methods in Molecular Biology. 1263, pp.243–250. DOI: 10.1007/978-1-4939-2269-7_19.

De Luca, L., 2006. Naturally occurring and synthetic imidazoles: their chemistry and their biological activities. *Current Medicinal Chemistry*, 13(1), pp.1–23.

Du, X., Li, Y., Xia, Y.L., Ai, S.M., Liang, J., Sang, P., Ji, X.L. & Liu, S.Q., 2016. Insights into protein–ligand interactions: mechanisms, models, and methods. *International Journal of Molecular Sciences*, 17(2), p.144. doi:10.3390/ijms17020144.

Ehret, G.B. & Caulfield, M.J., 2013. Genes for blood pressure: An opportunity to understand hypertension. *European Heart Journal*, 34(13), pp.951–961. DOI: 10.1093/eurheartj/ehs455.

European Society of Hypertension (ESH), 2023. 2023 ESH Guidelines for the management of arterial hypertension. *Journal of Hypertension*, 41(12), pp.1874–2000. DOI: 10.1097/HJH.0000000000003480.

Fajar, J.K., Pikir, B.S., Sidarta, E.P., Saka, P.N.B., Akbar, R.R., Tamara, F., Mayasari, E.D., Gunawan, A. & Heriansyah, T., 2019. The gene polymorphism of angiotensinogen (AGT) M235T and AGT T174M in patients with essential hypertension: A meta-analysis. *Gene Reports*, 16, p.100421. DOI: 10.1016/j.genrep.2019.100421.

Filippini, T., Naska, A., Kasdagli, M.I., Torres, D., Lopes, C., Carvalho, C., Moreira, P., Malavolti, M., Orsini, N., Whelton, P.K. & Vinceti, M., 2020. Potassium intake and blood pressure: A dose–response meta-analysis. *Journal of the American Heart Association*, 9(12), e015719. DOI: 10.1161/JAHA.119.015719.

Forli, S., Huey, R., Pique, M.E., Sanner, M.F., Goodsell, D.S. & Olson, A.J., 2016. Computational protein–ligand docking and virtual drug screening with the AutoDock suite. *Nature Protocols*, 11(5), pp.905–919. DOI: 10.1038/nprot.2016.051.

Frishman, W.H., 2013. β-Adrenergic blockade in cardiovascular disease. *Journal of Cardiovascular Pharmacology and Therapeutics*, 18, pp.310–319. https://api.semanticscholar.org/CorpusID:19506044

Frishman, W.H., 2013. β-Adrenergic blockade in cardiovascular disease. *Journal of Cardiovascular Pharmacology and Therapeutics*, 18, pp.310–319.

Global Burden of Disease Study, 2020. Global burden of 87 risk factors in 204 countries and territories, 1990–2019. *The Lancet*, 396(10258), pp.1223–1249. DOI: 10.1016/S0140-6736(20)30752-2.

Grassi, G., Seravalle, G., Quarti-Trevano, F., Dell'Oro, R. & Mancia, G., 2009. Sympathetic and baroreflex cardiovascular control in hypertension and hypotension. *Hypertension*, 53(2), pp.205–209. DOI: 10.1161/HYPERTENSIONAHA.108.121467.

Guyton, A.C., 1991. Blood pressure control—Special role of the kidneys and body fluids. *Science*, 252(5014), pp.1813–1816. DOI: 10.1126/science.2063193.

Hafez, A., Abdelaziz, A., Mansour, A., Kamal, I., Bakr, A., Gadelmawla, A.F., Elsayed, H., Mohamed, M.R., Ali, K. and Elhelw, M., 2025. Efficacy and safety of esaxerenone for essential hypertension: a systematic review and meta-analysis of randomized controlled trials. *Journal of Clinical Medicine*, 14(16), p.5663. https://doi.org/10.3390/jcm14165663

Hall, J.E., do Carmo, J.M., da Silva, A.A., Wang, Z. & Hall, M.E., 2015. Obesity-induced hypertension: Interaction of neurohumoral and renal mechanisms. *Circulation Research*, 116(6), pp.991–1006. DOI: 10.1161/CIRCRESAHA.116.305697.

Higashi, Y. & Chayama, K., 2002. Renal endothelial dysfunction and hypertension. *Journal of Diabetes and Its Complications*, 16(1), pp.103–107. DOI: 10.1016/S1056-8727(01)00202-1.

Ibrahim, S., Salama, I., Darweesh, K., Loksha, Y. & Kishk, S., 2024. A review: Imidazole and its biological activities. *Records of Pharmaceutical and Biomedical Sciences*, 8(1), pp.123–129. DOI: 10.21608/rpbs.2024.294154.1301.

Jain, A.K., Ravichandran, V., Sisodiya, M. and Agrawal, R.K., 2010. Synthesis and antibacterial evaluation of 2-substituted-4,5-diphenyl-N-alkyl imidazole derivatives. Asian Pacific Journal of Tropical Medicine, pp.471-474.

Kearney, P.M., Whelton, M., Reynolds, K., Muntner, P., Whelton, P.K. & He, J., 2005. Global burden of hypertension: Analysis of worldwide data. *Lancet*, 365, pp.217–222.

Kidney Disease: Improving Global Outcomes (KDIGO) Blood Pressure Work Group, 2021. KDIGO 2021 clinical practice guideline for the management of blood pressure in chronic kidney disease. *Kidney International*, 99(3S), pp.S1–S87. DOI: 10.1016/j.kint.2020.11.003.

Kim, G.-H., 2024. Primary role of the kidney in pathogenesis of hypertension. *Life*, 14(1), p.119. DOI: 10.3390/life14010119.

Kim, S., Chen, J., Cheng, T., et al., 2023. Nucleic Acids Research, 51(D1), pp.D1373–D1380. https://doi.org/10.1093/nar/gkac956

Kim, S., Thiessen, P.A., Bolton, E.E., et al., 2016. Nucleic Acids Research, 44(D1), pp.D1202–D1213. https://doi.org/10.1093/nar/gkv951

Kjeldsen, S.E., 2018. Hypertension and cardiovascular risk: General aspects. *Pharmacological Research*, 129, pp.95–99. doi.org/10.1016/j.phrs.2017.11.003

Lakshmi, P., Kamala, G. & Saraswathi, S., 2025. A review on advances computer-aided drug design and its applications in drug discovery: Review article. *Journal of Pharma Insights and Research*, 3(4), pp.062–069. DOI: 10.69613/9b88sm25.

Leelananda, S.P. & Lindert, S., 2016. Computational methods in drug discovery. *Beilstein Journal of Organic Chemistry*, 12, pp.2694–2718. DOI: 10.3762/bjoc.12.267.

Lindholm, L.H., Carlberg, B. & Samuelsson, O., 2005. Should β blockers remain first choice in the treatment of primary hypertension? A meta-analysis. *The Lancet*, 366(9496), pp.1545–1553. doi.org/10.1016/S0140-6736(05)67573-3

Lionta, E., Spyrou, G., Vassilatis, D.K. & Cournia, Z., 2014. Structure-based virtual screening for drug discovery: principles, applications and recent advances. *Current Topics in Medicinal Chemistry*, 14(16), pp.1923–1938. DOI: 10.2174/1568026614666140929124445.

Meng, X.-Y., Zhang, H.-X., Mezei, M. & Cui, M., 2011. Molecular docking: A powerful approach for structure-based drug discovery. *Current Computer-Aided Drug Design*, 7(2), pp.146–157. DOI: 10.2174/157340911795677602.

Mesas, A.E., Leon-Muñoz, L., Rodriguez-Artalejo, F. & Lopez-Garcia, E., 2011. The effect of coffee on blood pressure and cardiovascular disease in hypertensive individuals: A systematic review and meta-analysis. *American Journal of Clinical Nutrition*, 94(4), pp.1113–1126. DOI: 10.3945/ajcn.111.016667.

Messerli, F.H., Bangalore, S. & Bavishi, C., 2018. Angiotensin-converting enzyme inhibitors in hypertension: To use or not to use? *Journal of the American College of Cardiology*, 71(13), pp.1474–1482. doi.org/10.1016/j.jacc.2018.01.058

Mills, K.T., Stefanescu, A. & He, J., 2020. The global epidemiology of hypertension. *Nature Reviews Nephrology*, 16(4), pp.223–237. DOI: 10.1038/s41581-019-0244-2.

Moitessier, N., Englebienne, P., Lee, D., Lawandi, J. & Corbeil, C.R., 2008. Towards the development of universal, fast and highly accurate docking/scoring methods: a long way to go. *British Journal of Pharmacology*, 153(S1), pp.S7–S26. DOI: 10.1038/sj.bjp.0707515.

Morris, G.M. & Lim-Wilby, M., 2008. *Molecular docking*. Methods in Molecular Biology, 443, pp.365–382. DOI: 10.1007/978-1-59745-177-2_19.

Mumtaz, A., Saeed, A., Fatima, N., Dawood, M., Rafique, H. & Iqbal, J., 2023. Imidazole and its derivatives as potential candidates for drug development. *Bangladesh Journal of Pharmacology*, 11(4). https://doi.org/10.3329/bjp.v11i4.26835

Ogah, O.S., Okpechi, I., Chukwuonye, I.I., Akinyemi, J.O., Onwubere, B.J., Falase, A.O., Stewart, S. & Sliwa, K., 2012. Blood pressure, prevalence of hypertension and hypertension-related complications in Nigerian Africans: A review. *World Journal of Cardiology*, 4(12), pp.327–340. DOI: 10.4330/wjc.v4.i12.327.

Oparil, S., Acelajado, M.C., Bakris, G.L., Berlowitz, D.R., Cífková, R., Dominiczak, A.F. & Whelton, P.K., 2018. Hypertension. *Nature Reviews Disease Primers*, 4(1), p.18014. DOI: 10.1038/nrdp.2018.14.

Pagadala, N.S., Syed, K. & Tuszynski, J., 2017. Software for molecular docking: A review. *Biophysical Reviews*, 9(2), pp.91–102. DOI: 10.1007/s12551-016-0247-1.

Parmar, M.B., Vara, M.K. & Pandya, J.H., 2024. A brief review on imidazole, triazine, and isatin derivatives: synthesis approaches and their applications. *Discover Chemistry*, 1(56). https://doi.org/10.1007/s44371-024-00057-z

Peixoto, A.J., 2019. Acute severe hypertension. *The New England Journal of Medicine*, 381(19), pp.1843–1852. DOI: 10.1056/NEJMcp1901117.

Pinna, G., Pascale, C., Fornengo, P., Arras, S., Piras, C., Panzarasa, P., Carmosino, G., Franza, O., Semeraro, V., Lenti, S., Pietrelli, S., Panzone, S., Bracco, C., Fiorini, R., Rastelli, G., Bergandi, D., Zampaglione, B., Musso, R., Marengo, C., Santoro, G., Zamboni, S., Traversa, B., Barattini, M. & Bruno, G., 2014. Hospital admissions for hypertensive crisis in the emergency departments: A large multicenter Italian study. *PLoS ONE*, 9(4), e93542. DOI: 10.1371/journal.pone.0093542.

Primatesta, P., Falaschetti, E., Gupta, S., Marmot, M.G. & Poulter, N.R., 2001. Association between smoking and blood pressure: Evidence from the Health Survey for England. *Hypertension*, 37(2), pp.187–193. DOI: 10.1161/01.hyp.37.2.187.

Raina, R., Nair, N., Chakraborty, R., Nemer, L., Dasgupta, R., Varian, K. et al., 2020. An update on the pathophysiology and treatment of cardiorenal syndrome. *Cardiology Research*, 11(2), pp.76–88. DOI: 10.14740/cr955.

Rama Brahma Reddy, D., Malleswari, K., Sreenivasulu, G. & Naga Sai, G., 2022. Imidazole derivatives and its pharmacological activities. *International Journal of Research and Analytical Reviews*, 9(4), pp.98–107.

Rehm, J., Roerecke, M., Kaczorowski, J., Tobe, S.W., Gmel, G. & Hasan, O.S.M., 2017. The effect of alcohol on blood pressure: A systematic review and meta-analysis. *Lancet Public Health*, 2(2), e108–e120. DOI: 10.1016/S2468-2667(17)30003-8.

Ritz, E., Fliser, D. & Siebels, M., 1993. Pathophysiology of hypertensive renal damage. *American Journal of Hypertension*, 6(7 Pt 2), pp.241S–244S. DOI: 10.1093/ajh/6.7.241s.

Roerecke, M., et al., 2017. The effect of alcohol on blood pressure: A systematic review and meta-analysis. *Lancet Public Health*, 2(2), e108–e120. DOI: 10.1016/S2468-2667(17)30003-8.

Rose, P.W., Prlić, A., Altunkaya, A., Bi, C., Bradley, A.R., Christie, C.H., … & Burley, S.K., 2017. The RCSB Protein Data Bank: Integrative view of protein, gene and 3D structural information. *Nucleic Acids Research*, 45(D1), D271–D281. https://doi.org/10.1093/nar/gkw1000

Safar, M.E., London, G.M. & Plante, G.E., 2004. Arterial stiffness and kidney function. *Hypertension*, 72(4), pp.163–168. DOI: 10.1161/01.HYP.0000114571.75762.b0.

Santos, K.B., Guedes, I.A., Karl, A.L.M. & Dardenne, L.E., 2019. Highly flexible ligand docking: Benchmarking of AutoDock and AutoDock Vina. *Journal of Chemical Information and Modeling*, 59(8), pp.3370–3388. DOI: 10.1021/acs.jcim.9b00905.

Saxena, T., Ali, A.O. & Saxena, M., 2018. Pathophysiology of essential hypertension: An update. *Expert Review of Cardiovascular Therapy*, 16(12), pp.879–887. DOI: 10.1080/14779072.2018.1540301.

Schlaich, M.P., Almahmeed, W., Arnaout, S., Prabhakaran, D., Zhernakova, J., Zvartau, N. & Schutte, A.E., 2020. The role of selective imidazoline receptor agonists in modern hypertension management: An international real-world survey (STRAIGHT). *Current Medical Research and Opinion*, 36(12), pp.1939–1945. https://doi.org/10.1080/03007995.2020.1835852

Schlaich, M.P., Tsioufis, K., Taddei, S., Ferri, C., Cooper, M., Sindone, A., Borghi, C., Parissis, J., Marketou, M., Vintila, A.M., Farcas, A., Kiuchi, M.G. & Chandrappa, S., 2024. Targeting the sympathetic nervous system with the selective imidazoline receptor agonist moxonidine for the management of hypertension: An international position statement. *Journal of Hypertension*, 42(12), pp.2025–2040. doi:10.1097/HJH.0000000000003769.

Schneider, G. & Fechner, U., 2005. Computer-based de novo design of drug-like molecules. *Nature Reviews Drug Discovery*, 4(8), pp.649–663. DOI: 10.1038/nrd1799.

Singh, N., 2017. A review on hypertensive analytics. *Der Pharma Chemica*, 9(14), pp.41–49.

Singh, R.B., Suh, I.L., Singh, V.P., Chaithiraphan, S., Laothavorn, P. & Sy, R.G., 2000. Hypertension and stroke in Asia: Prevalence, control and strategies in developing countries for prevention. *Journal of Human Hypertension*, 14, pp.749–763.

Spruill, T.M., 2010. Chronic psychosocial stress and hypertension. *Current Hypertension Reports*, 12(1), pp.10–16. DOI: 10.1007/s11906-009-0084-8.

Taddei, S., Virdis, A., Ghiadoni, L., Magagna, A. & Salvetti, A., 2000. Endothelial dysfunction in hypertension. *Journal of Nephrology*, 13(3), pp.205–210.

Taylor, A.A., 2001. Pathophysiology of hypertension and endothelial dysfunction in patients with diabetes mellitus. *Endocrinology and Metabolism Clinics of North America*, 30(4), pp.983–997. DOI: 10.1016/s0889-8529(05)70223-1.

Trott, O. & Olson, A.J., 2009. AutoDock Vina: Improving the speed and accuracy of docking with a new scoring function, efficient optimization, and multithreading. *Journal of Computational Chemistry*, 31(2), pp.455–461. doi:10.1002/jcc.21334.

Trott, O. & Olson, A.J., 2010. AutoDock Vina: Improving the speed and accuracy of docking with a new scoring function, efficient optimization, and multithreading. *Journal of Computational Chemistry*, 31(2), pp.455–461. DOI: 10.1002/jcc.21334.

Vilela-Martin, J.F., Vaz-de-Melo, R.O., Kuniyoshi, C.H., Abdo, A.N. & Yugar-Toledo, J.C., 2011. Hypertensive crisis: Clinical-epidemiological profile. *Hypertension Research*, 34(3), pp.367–371. DOI: 10.1038/hr.2010.245.

Virdis, A., Giannarelli, C., Neves, M.F., Taddei, S. & Ghiadoni, L., 2010. Cigarette smoking and hypertension. *Current Pharmaceutical Design*, 16(23), pp.2518–2525. DOI: 10.2174/138161210791959820.

Whelton, P.K., Carey, R.M., Aronow, W.S. et al., 2018. 2017 ACC/AHA/AAPA/ABC/ACPM/AGS/APhA/ASH/ASPC/NMA/PCNA guideline for the prevention, detection, evaluation, and management of high blood pressure in adults. *Journal of the American College of Cardiology*, 71(19), pp.e127–e248. DOI: 10.1016/j.jacc.2017.11.006.

Williams, B., Mancia, G., Spiering, W., Agabiti Rosei, E., Azizi, M., Burnier, M., Coca, A. et al., 2018. 2018 ESC/ESH Guidelines for the management of arterial hypertension. *European Heart Journal*, 39(33), pp.3021–3104. DOI: 10.1093/eurheartj/ehy339.

World Health Organization (WHO), 2023. Hypertension fact sheet. [online] Available at: https://www.who.int/news-room/fact-sheets/detail/hypertension [Accessed 8 November 2025].

Zhang, L., Peng, X.M., Damu, G.L., Geng, R.X. & Zhou, C.H., 2014. Comprehensive review in current developments of imidazole-based medicinal chemistry. *Medical Research Reviews*, 34(2), pp.340–437. doi:10.1002/med.21290.

Zhou, J., Ji, M., Zhu, Z., Cao, R., Chen, X. & Xu, B., 2017. Discovery of 2-substituted 1H- benzo[d]imidazole- 4- carboxamide derivatives as novel poly(ADP- ribose) polymerase- 1 inhibitors with in vivo anti-tumor activity. *European Journal of Medicinal Chemistry*, 132, pp.26–41. DOI: 10.1016/j.ejmech.2017.03.013.

APPENDIX

Calculation of theoretical yield and percentage yield

Compound: 2,4,5-triphenyl-1H-imidazole

Reagents used: benzil (2.625 g), benzaldehyde (1.27 mL)

Assumed reaction stoichiometry: 1 mole benzil + 1 mole benzaldehyde → 1 mol product (2,4,5-triphenyl-1H-imidazole)

1. Molar masses

- Benzil, $C_{14}H_{10}O_2$:

  Molecular Mass of Benzil=210.234 g\mol
- Benzaldehyde, C_7H_6O:

  Molecular Mass Benzaldehyde=106.12 g\mol
- Density of benzaldehyde (used to convert volume → mass):

  Density of Benzaldehyde=1.044 g\ml
- 2,4,5-Triphenyl-1H-imidazole (product):

  Molecular Mass of Product=296.373 g\mol

2. Stepwise calculation

Moles of benzil used

$$\text{Mole of benzil} = \frac{\text{Mass}}{\text{Molar mass}} = \frac{2.625\text{g}}{210.23\ \text{g/mol}} = 0.0125\text{mol}$$

Mass of Benzaldehyde:

Mass of Benzaldehyde = Density × Volume = 1.26 mL × 1.044 g/mL-1 = 1.326 g

Moles of Benzaldehyde:

$$\text{Moles of Benzaldehyde} = \frac{\text{Mass}}{\text{Molar mass}} = \frac{1.326\text{g}}{106.12\ \text{g/mol}} = 0.0125\text{mol}$$

Theoretical mass (theoretical yield) of product

$$\text{Theoretical yield} = \frac{\text{Mass of Benzaldehyde} \times \text{ Molar Mass of Product}}{\text{Molar Mass Benzaldehyde}} = \frac{1.326 \times 296.37}{106.12}$$

$$= 3.70g$$

Theoretical yield = 3.703 g

3. Determination of Percentage yield

Percentage yield is calculated as:

$$\%\ yield = \frac{Actual\ yield}{Theoritical\ Yield} \times 100\%$$

Using the theoretical yield found above:

$$\%\ yield = \frac{3.01g}{3.703} \times 100\% = 81.28\%$$